

SUPPORTING INFORMATION

Epigenetic determinants of ovarian clear cell carcinoma biology

Ken Yamaguchi^{1,2}, Zhiqing Huang¹, Noriomi Matsumura², Masaki Mandai³, Zhiqing Huang¹, Takako Okamoto², Tsukasa Baba², Ikuo Konishi², Andrew Berchuck¹ and Susan K. Murphy¹

¹ Department of Obstetrics and Gynecology, Duke University Medical Center, Durham NC, USA

² Department of Gynecology and Obstetrics, Graduate School of Medicine, Kyoto University, Kyoto, Japan

³ Department of Obstetrics and Gynecology, Kinki University Faculty of Medicine, Osaka, Japan

Cell Lines and Clinical Samples

The immortalized human ovarian surface epithelial (OSE) cell line HOSE/E7/hTERT was kindly provided by Dr. Hidetaka Katabuchi at Kumamoto University and was maintained as described ¹. The other immortalized OSE cell lines, IOSE80 and IOSE114, were kindly provided by Dr. Mythreye Karthikeyan at Duke University and were cultured as described ^{2,3}. The endometriosis cell line Hs832(c)T (derived from an ovarian endometriotic cyst) was purchased from the American Type Culture Collection (ATCC) and was cultured according to their protocol. Ovarian cancer cell lines, including 14 CCC and 32 non-CCC cell lines (Supplementary Table 1), were cultured in RPMI1640 media (Sigma-Aldrich Co., St. Louis, MO) supplemented with penicillin and streptomycin (100 U/mL penicillin, 100 µg/mL streptomycin; Invitrogen, Carlsbad, CA) and 10% heat inactivated fetal bovine serum (v/v; Invitrogen), RPMI1640/FBS/pen-strep medium, in an atmosphere of 5% CO₂ at 37°C. The short tandem repeat (STR) genotypes of all ovarian cancer cell lines were analyzed to authenticate the cell lines using either the PowerPlex[®] 1.2 System (Promega, Madison, WI) at The Fragment Analysis Facility of Johns Hopkins University or the AmpF ℓ STR[®] Identifier[®] Plus PCR Amplification Kit (Applied Biosystems, Carlsbad, CA) at the University of Colorado Cancer Center, DNA Sequencing and Analysis Core. The STR genotypes of ovarian cancer cell lines that are available from ATCC, RIKEN BioResource Center Cell Bank, or the Japanese Collection of Research Bioresources (JCRB) Cell Bank were identical to the source genotypes as reported within their respective STR databases and all

other non-commercially available cell lines were shown to be derived from females with unique genotypes.

Tissue specimens were derived from 85 patients with ovarian cancer treated at Duke University Medical Center, all of whom provided written informed consent (13 CCC, 53 SAC, 11EAC, and 8 MAC) and from eight patients without malignant disease (4 ovarian surface epithelium samples and 4 fallopian tube epithelium samples). Frozen tissue samples were embedded in optimal cutting temperature medium, and were stored at -80°C . All sections were cut and mounted on slides to confirm that at least 60% of the cellular content comprised cancer cells with less than 20% necrosis. Tumors were histologically classified according to World Health Organization (WHO) criteria. Clinical staging was performed according to the International Federation of Obstetrics and Gynecology (FIGO) criteria. Evaluation was performed by two independent pathologists in the absence of clinical information.

Extraction of Genomic DNA and Bisulfite Treatment

Genomic DNA was extracted from cells cultured in a 10 cm dish when they reached 70-90% confluence using the QIAamp[®] DNA Mini Kit (Qiagen Inc., Valencia, CA) or from 5-20 mg of clinical tissues using the AllPrep[®] DNA/RNA/Protein Mini Kit (Qiagen Inc.). DNA quality and quantity were determined using a NanoDrop ND-1000 (Thermo Fisher Scientific, Wilmington, DE). Five hundred ng of genomic DNA with both A_{260}/A_{280} and $A_{260}/A_{230} \geq 1.7$ were bisulfite modified using the EZ DNA Methylation[™] Kit (Zymo Research Co., Irvine, CA) according to the manufacturer's protocol for the Infinium

methylation assay, and 800 ng of genomic DNA was bisulfite modified using the same kit but according to standard protocol for methylation analysis of individual genes.

Illumina Infinium HumanMethylation BeadChip Assay

Genomic DNA was bisulfite modified using the EZ DNA Methylation Kit (Zymo Research; Irvine, CA). Bisulfite-converted genomic DNA was analyzed using Illumina's Infinium HumanMethylation27 BeadChip for cell line samples and HumanMethylation450 Beadchip for clinical tissue specimens (Illumina Inc., San Diego, CA). The HumanMethylation27 BeadChip contains 27,578 CpG loci covering 14,495 gene IDs as annotated by Illumina. The majority of the CpG dinucleotides on this platform (26,956; 97.7%) are located in close proximity to gene promoters with 20,006 (72.5%) located within CpG islands. The HumanMethylation450 BeadChip contains 485,836 CpG sites including those within CpG islands and in CpG island shores and shelves⁴, intergenic and intragenic CpG sites as well as CpGs identified as differentially methylated between tumor versus normal tissues. The HumanMethylation450 BeadChip includes 90% of the content contained on the HumanMethylation27 BeadChip. Chip processing was performed according to the manufacturer's protocol by Expression Analysis Inc., (Durham, NC), an Illumina Certified Service Provider. Data were extracted using Illumina[®] GenomeStudio[™] v2010.3 software (Illumina Inc.). Methylation values for each CpG locus are represented as β -values, a quantitative measure of DNA methylation, with levels ranging from 0 (completely unmethylated) to 1 (completely methylated). CpGenome Universal Methylated

DNA (Millipore Co., Billerica, MA) was used as a positive control. Other controls included human normal lymphocyte genomic DNA and a 50:50 mixture of the CpGenome Universal Methylated DNA and human normal lymphocyte genomic DNA. Replicate samples (N=6) were included on each of the six BeadChips run for the HumanMethylation27 BeadChip analysis to assess inter-chip reproducibility ($r > 0.9991$, $p < 0.000001$). Bisulfite conversion efficiency (i.e., the conversion of non-CpG cytosines to uracils) was assessed for all samples by Pyrosequencing (see below) prior to data generation using the Illumina BeadChips. At two independent chromosomal loci (*BRCA1* and *IGF2* for cell line samples, and *HNF1B* and *F2* for clinical tissues), average bisulfite conversion efficiency for all samples was 98.83% (+/-0.54% SD) for cell lines and 99.20% (+/-1.28% SD) for clinical tissues. We opted to use raw data for our analysis since the methylation levels as detected by quantitative bisulfite pyrosequencing were very strongly correlated with the methylation beta-values as detected on the HumanMethylation450 platform ($0.939 < r < 0.981$, $p < 0.000001$ for all genes analyzed; data not shown)

Methylation Specific Polymerase Chain Reaction (MS-PCR)

The DNA methylation status of estrogen receptor alpha (ERalpha) network genes (*ESR1*, *BMP4*, *DKK1*, *SOX11*, *SNCG* and *MOSCI*) was validated using MS-PCR. 46 cell lines (14 CCC and 32 non-CCC) and 84 (13 CCC and 71 non-CCC) clinical specimens were used for analysis. Genomic DNA (~800 ng) was modified with sodium bisulfite using the EZ DNA Methylation Kit (Zymo Research). Primer sequences and PCR conditions are shown in Supplemental Table 2a. Primers were designed such that they annealed to

sequence containing the CpG site analyzed for the given gene on the HumanMethylation450 beadchip, or were as close as possible to these CpG sites. HotStarTaq[®] DNA Polymerase (Qiagen) was used for MS-PCR with 20 ng of bisulfite modified DNA (EZ DNA Methylation Kit; Zymo Research) in a 12.5 µl reaction volume with 2 mM MgCl₂, 10.4 mM dNTPs and 0.4 µM each primer. Cycling conditions included a 95°C incubation for 15 minutes followed by denaturation at 94°C for 30 seconds, annealing at the temperatures listed in Supplementary Table 2a for 30 seconds, and extension at 72°C for 30 seconds for the cycle number indicated in Supplementary Table 2a, followed by a 10 minute final extension at 72°C. The amplicons were resolved on 2% agarose gels and visualized by ethidium bromide staining. Specimens analyzed were scored as “methylated” if there were amplicons produced by the primers specific to the methylated sequence or by both the methylated and unmethylated sets of primers, or as “unmethylated” when amplicons were produced only from the primer set specific to the unmethylated sequence. Controls included bisulfite modified CpGenome Universal Methylated DNA (Millipore Co.), human normal lymphocyte genomic DNA and a 50:50 mixture of these DNAs.

Pyrosequencing

All primers for pyrosequencing assays were designed using PSQ assay design software version 1.0.6 (Biotage, Uppsala, Sweden). The pyrosequencing assays were designed such that we could analyze the same CpG sites as those present on the Illumina BeadChip for eleven genes (*ESR1*, *HNF1A*, *HNF1B*, *C14orf105*, *KIF12*, *MIA2*, *PAX8*,

SERPINA6, *SGK2*, *SRC* and *TM4SF4*) and adjacent CpG sites for the *F2* gene. Primer sequences and PCR conditions are shown in Supplemental Table 2b. PCR was performed using ~40 ng of bisulfite modified genomic DNA as template per reaction (EZ DNA Methylation Kit; Zymo Research) with the PyroMark PCR Master Mix (Qiagen). Pyrosequencing was conducted using PyroMark Gold Q98 Reagents (Qiagen). Methylation values for each CpG site were calculated using Pyro Q-CpG software 1.0.9 (Biotage). The ten genes for which identical CpG sites were analyzed for validation purposes showed very strong positive correlations between the Infinium assay β -values and the percent methylation as measured by pyrosequencing ($r > 0.9605$, $p < 0.000001$ for all genes; Supplementary Figure 3). Adjacent CpG sites for these same ten genes also showed significant positive correlations between the β -values of the Infinium assay CpG sites and the percent methylation by pyrosequencing, as did the adjacent CpG sites measured for the *F2* gene ($0.7498 < r < 0.9813$, $p < 0.000001$ for all genes; Supplementary Figure 4).

Real Time Polymerase Chain Reaction (RT-PCR)

Two micrograms of total RNA prepared from 36 ovarian cancer cell lines (13 CCC, 13 SAC, 3 EAC, 4 MAC and 3 others) or 49 frozen tissues (13 CCC, 18 SAC, 12 EAC and 6 MAC) were used to generate cDNA in a 40 μ l volume with the Superscript II kit (Invitrogen). Two μ l of the cDNA was used as template for real time PCR on an Applied Biosystems 7900HT Fast Real Time PCR instrument and TaqMan Assays on Demand per the manufacturer's instructions (Applied Biosystems) except that a 20 μ l reaction volume was used. Genes analyzed were *HNF1B* (Assay ID Hs01001602), *C14orf105*

(Hs00216847), *SGK2* (Hs00367639), *F2* (Hs01011988), *ESR1* (Hs00174860), *CRIP1* (Hs00832816), *SOX11* (Hs00846583), *IGFBP4* (Hs01057900) and *BMP4* (Hs00370078).

Expression of *B2M* (Hs 00187842) was measured in parallel for each specimen and used as a control for RNA input. Relative expression was calculated using the delta delta Ct method.

5-Aza-2'-Deoxycytidine (Decitabine) Treatment

RMG-2, RMG-5, and KOC-7C cell lines were cultured in RPMI1640 media (Sigma-Aldrich Co., St. Louis, MO) supplemented with penicillin and streptomycin (100 U/mL penicillin, 100 µg/mL streptomycin; Invitrogen) and 10% heat inactivated fetal bovine serum (v/v; Invitrogen) in an atmosphere of 5% CO₂ at 37°C. The cells were trypsinized and seeded into a 6-well plate. The following day the cells were treated in triplicate by adding RPMI1640/FBS/pen-strep media (mock) or the same media containing 5µM 5-aza-2'-deoxycytidine (Decitabine; Sigma-Aldrich Co). The media was replaced daily (with/without Decitabine as relevant) for three days after which the cells had reached 70% to 90% confluence and were harvested for DNA extraction as described above or RNA extraction using RNA Stat60 (Teltest; Friendswood TX). Real time RT-PCR and pyrosequencing analysis were performed as described above.

Bioinformatics

Identification of genes showing differential methylation

Identification of genes that show different methylation levels between groups was

done by comparing the β -values of these groups using unpaired t-tests with thresholds of $p < 0.01$ and difference of average β -values > 0.2 (20% methylation) for the comparison between ovarian cancer cell lines and normal cells or between CCC and non-CCC. Genes annotated by gene name or gene ID (Illumina annotation file) were used for the analyses.

Unsupervised consensus clustering

For evaluation of the similarity between genes or specimens, consensus clustering was applied to divide the data successively into $k = 2, 3, 4 \dots$ clusters, with 80% bootstrapping of 300 subsamples of genes and/or samples using ConsensusCluster software⁵. All CpG sites on the HumanMethylation27 BeadChip (27,578 CpG sites) were analyzed and the CpG sites annotated by gene name on the HumanMethylation450 BeadChip. These were filtered to include those showing standard deviations of β -values > 0.1 across samples (135,945 CpG sites) which were then used for unsupervised consensus clustering. All samples were divided into five clusters using K-Means clustering⁵.

Identification of genes regulated by DNA methylation in ovarian cancer

Two cell line microarray datasets [Gene Expression Omnibus (GEO) Accession Number: GSE25428 and GSE29175^{6,7}] were used for the identification of candidate genes whose mRNA expression levels are regulated by DNA methylation in ovarian cancer. The ComBat normalizing algorithm was used before performing any analysis to reduce the likelihood of batch effects⁸. Candidate genes functionally regulated by methylation were identified based on the following criteria: 1) the p-value of unpaired Student t-tests is less

than 0.01; 2) the average β -value difference is more than 0.2 (20% methylation) between 14 CCC cell lines and 32 non-CCC cell lines; and 3) a significant inverse correlation ($p < 0.05$) between expression microarray values and β -values from the Infinium assay for the 42 ovarian cancer cell lines with gene expression data. First, 856 genes (1 042 CpG sites) showed increased methylation, and 44 genes (54 CpG sites) showed decreased methylation in CCC as compared to non-CCC (Supplementary Figure 2a). Next, potential functional relationships between expression and methylation of the 856 HM and 44 UM CCC genes was assessed by determining if there were correlations between these values. Of 625 evaluable HM genes, 276 genes showed a significant inverse correlation ($r < -0.3051$, $p < 0.05$) between methylation and expression. Of the 33 evaluable UM genes, 22 showed a significant inverse correlation ($r < -0.3217$, $p < 0.05$) between methylation and expression (Supplementary Figure 2b). Published expression microarray datasets representing clinical ovarian cancer samples (GSE6008 and GSE2109) were used for external validation^{9, 10}. Genes transcriptionally regulated by DNA methylation were used to conduct average-linkage hierarchical clustering of GSE6008 and GSE2109 datasets with Cluster version 3.0. (<http://rana.lbl.gov/eisen/>). Only the overlapping probe sets between the U133A and U133 plus 2.0 dataset (GSE2109) were used. For all analyses, levels of gene expression were standardized using mean-centering. Heat maps and dendrograms were generated with Java TreeView (<http://jtreeview.sourceforge.net/>).

Categorical Analyses

The biological characteristics of the CCC-specific methylation signature were

evaluated using the enrichment of Molecular Signatures Database (MSigDB) gene sets (v2.5 updated April 7 2008) ¹¹ with the R package *allez* 1.0 ¹². Briefly, for each gene set, the proportion of the annotated genes in the CCC hypermethylated or hypomethylated gene sets was compared to that for all probeset genes. A gene set was considered significantly enriched if the z-score was more than 4.0 ¹³.

Pathway Analyses

The relationship of hypermethylated or hypomethylated genes to particular pathways was evaluated using MetaCore™ software. (GeneGo; <http://www.genego.com/>), an integrated knowledge database and software suite for evaluation of the association between a particular gene list and known pathways.

Heatmap of beta-values and expression

Absolute beta-values are represented by color gradient intensity, from white; beta-value =0, to red; beta-value =1, using Java TreeView (<http://jtreeview.sourceforge.net/>). Average-linkage hierarchical clustering was performed in GSE6008 and GSE2109 (clinical ovarian cancer datasets) expression datasets using genes transcriptionally regulated by DNA methylation with Cluster version 3.0. (<http://rana.lbl.gov/eisen/>). For all analyses, levels of gene expression were standardized using mean-centering. Heatmaps and dendrograms were generated with Java TreeView.

Statistical Analyses

The Mann-Whitney test was used to compare continuous variables between groups. Fisher's exact test was used for analysis of categorical variables. Correlations between expression microarray values and methylation beta-values from the Infinium assay or between beta-values and % methylation values from pyrosequencing were evaluated using Pearson's correlation. P-values less than 0.05 were considered statistically significant.

References

1. Maeda T, Tashiro H, Katabuchi H, Begum M, Ohtake H, Kiyono T, Okamura H. Establishment of an immortalised human ovarian surface epithelial cell line without chromosomal instability. *British Journal of Cancer* 2005;93:116-23.
2. Maines-Bandiera SL, Kruk PA, Auersperg N. Simian virus 40-transformed human ovarian surface epithelial cells escape normal growth controls but retain morphogenetic responses to extracellular matrix. *Am J Obstet Gynecol* 1992;167:729-35.
3. Auersperg N, Maines-Bandiera SL, Dyck HG, Kruk PA. Characterization of cultured human ovarian surface epithelial cells: phenotypic plasticity and premalignant changes. *Lab Invest* 1994;71:510-8.
4. Irizarry RA, Ladd-Acosta C, Wen B, Wu Z, Montano C, Onyango P, Cui H, Gabo K, Rongione M, Webster M, Ji H, Potash JB, et al. The human colon cancer methylome shows similar hypo- and hypermethylation at conserved tissue-specific CpG island shores. *Nat Genet* 2009;41:178-86.
5. Seiler M, Huang CC, Szalma S, Bhanot G. ConsensusCluster: a software tool for unsupervised cluster discovery in numerical data. *OMICS* 2010;14:109-13.
6. Matsumura N, Huang Z, Mori S, Baba T, Fujii S, Konishi I, Iversen ES, Berchuck A, Murphy SK. Epigenetic suppression of the TGF-beta pathway revealed by transcriptome profiling in ovarian cancer. *Genome Res* 2010.
7. Yamaguchi K, Mandai M, Oura T, Matsumura N, Hamanishi J, Baba T, Matsui S, Murphy SK, Konishi I. Identification of an ovarian clear cell carcinoma gene signature that

reflects inherent disease biology and the carcinogenic processes. *Oncogene* 2010;29:1741-52.

8. Johnson WE, Li C, Rabinovic A. Adjusting batch effects in microarray expression data using empirical Bayes methods. *Biostatistics* 2007;8:118-27.

9. Marquez RT, Baggerly KA, Patterson AP, Liu J, Broaddus R, Frumovitz M, Atkinson EN, Smith DI, Hartmann L, Fishman D, Berchuck A, Whitaker R, et al. Patterns of gene expression in different histotypes of epithelial ovarian cancer correlate with those in normal fallopian tube, endometrium, and colon. *Clin Cancer Res* 2005;11:6116-26.

10. Wu R, Hendrix-Lucas N, Kuick R, Zhai Y, Schwartz DR, Akyol A, Hanash S, Misek DE, Katabuchi H, Williams BO, Fearon ER, Cho KR. Mouse model of human ovarian endometrioid adenocarcinoma based on somatic defects in the Wnt/beta-catenin and PI3K/Pten signaling pathways. *Cancer Cell* 2007;11:321-33.

11. Subramanian A, Tamayo P, Mootha VK, Mukherjee S, Ebert BL, Gillette MA, Paulovich A, Pomeroy SL, Golub TR, Lander ES, Mesirov JP. Gene set enrichment analysis: a knowledge-based approach for interpreting genome-wide expression profiles. *Proc Natl Acad Sci U S A* 2005;102:15545-50.

12. Newton MA, Quintana FA, den Boon JA, Sengupta S, Ahlquist P. Random-set methods identify distinct aspects of the enrichment signal in gene-set analysis. *Annals of Applied Statistics* 2007;1:85-106.

13. Pyeon D, Newton MA, Lambert PF, den Boon JA, Sengupta S, Marsit CJ, Woodworth CD, Connor JP, Haugen TH, Smith EM, Kelsey KT, Turek LP, et al. Fundamental differences in cell cycle deregulation in human papillomavirus-positive and

human papillomavirus-negative head/neck and cervical cancers. *Cancer Res* 2007;67:4605-

19.

Supplementary Table 1 Cell Lines						
#	Name	Organ-Histology	46 OvCa^a	42 OvCa^b	36 OvCa^c	Source^d
1	41M	SAC	1	1		Kyoto Univ.
2	A2780-NCI	adenocarcinoma	1		1	ATCC
3	Caov-3	SAC	1	1	1	Duke
4	DOV13	adenocarcinoma	1	1		Duke
5	ES-2	CCC	1			ATCC
6	FUOV1	SAC	1	1		Duke
7	Hey	SAC	1	1	1	Duke
8	IGROV1-NCI	EAC	1		1	ATCC
9	JHOC-5	CCC	1	1	1	Riken
10	JHOC-7	CCC	1	1	1	Riken
11	JHOC-8	CCC	1	1	1	Riken
12	JHOC-9	CCC	1	1	1	Riken
13	JHOM-1	MAC	1	1	1	Riken
14	JHOM-2B	MAC	1	1	1	Riken
15	JHOS-2	SAC	1	1	1	Riken
16	JHOS-3	SAC	1	1	1	Riken
17	JHOS-4	SAC	1	1	1	Riken
18	KOC-5c	CCC	1	1	1	Kurume Univ.
19	KOC-7c	CCC	1	1	1	Tottori Univ.
20	MCAS	MAC	1	1	1	Kyoto Univ.
21	OVCAR-3	Undifferentiated	1	1	1	Duke
22	OMC-3	MAC	1	1	1	Riken
23	OV90	SAC	1	1	1	Duke
24	ovary1847	SAC	1	1	1	Duke
25	OVCA420	SAC	1	1	1	Duke
26	OVCA429	SAC	1	1	1	Duke
27	OVCA432	SAC	1	1	1	Duke
28	OVCAR2	adenocarcinoma	1	1		Duke
29	OVCAR4-NCI	adenocarcinoma	1			ATCC
30	OVCAR5	adenocarcinoma	1	1		Duke
31	OVCAR8	adenocarcinoma	1	1	1	Duke
32	OVISE	CCC	1	1	1	Yokohama City Univ.
33	OVK-18	EAC	1	1	1	Riken
34	OVTOKO	CCC	1	1	1	Yokohama City Univ.
35	PA1	Teratocarcinoma	1	1		Duke
36	PEO1	SAC	1	1	1	Duke

37	RMG-I	CCC	1	1	1	Keio Univ.
38	RMG-II	CCC	1	1	1	Keio Univ.
39	RMG-V	CCC	1	1	1	Keio Univ.
40	SK-OV-3	SAC	1	1	1	Duke
41	SK-OV-8	unknown	1	1		Duke
42	TAYA	CCC	1	1	1	Jichi Medical Univ.
43	TOV-112D	EAC	1	1	1	Duke
44	TOV-21G	CCC	1	1	1	Duke
45	TYK-nu	Undifferentiated	1	1	1	Kyoto Univ.
46	UWB1.289	SAC	1			ATCC
47	HOSE/E7/hTERT	Immortalized ovarian surface epithelium (normal)				Kumamoto Univ.
48	IOSE80	Immortalized ovarian surface epithelium (normal)				Duke
49	IOSE144	Immortalized ovarian surface epithelium (normal)				Duke
50	Hs832.(C)T	Endometriosis (normal)				ATCC
2'	A2780-J	adenocarcinoma		1		Kyoto Univ.

a. Used for the identification of differentially methylated genes

b. Used for a calculation of inverse correlation between expression values and beta-values

c. Used for RT-PCR

d. ATCC: the American Type Culture Collection

Riken: RIKEN BioResource Center Cell Bank

Kuruma Univ., Tottori Univ., Yokohama City Univ., Keio Univ., Jichi Medical Univ., and

Kumamoto Univ. kindly provided cell lines for us.

Supplementary Table 2a MS-PCR primers			
Gene Name	Primers	Primer Sequences	Annealing
<i>ESR1</i>	Methylated Forward	CGAGTTGGAGTTTTTGAATCGTTC	57 °C x 40
	Methylated Reverse	CTACGCGTTAACGACGACCG	
	Unmethylated Forward	ATGAGTTGGAGTTTTTGAATTGTTT	57 °C x 35
	Unmethylated Reverse	ATAAACCTACACATTAACAACAACCA	
<i>BMP4</i>	Methylated Forward	TTTGCGTAGAGCGATTTACGCGC	73 °C x 5 >
	Methylated Reverse	CTTCCTCCRTTACACCAACAACA	70 °C x 5 >
	Unmethylated Forward	GGTTTTTGTGTAGAGTGATTTATGTGT	67 °C x 5 >
	Unmethylated Reverse	CTTCCTCCRTTACACCAACAACA	64 °C x 30
<i>DKK1</i>	Methylated Forward	GTCGGAATGTTTCGGGTTTCGC	72 °C x 5 >
	Methylated Reverse	AAACCTAAATCCCCACGAAAC	70 °C x 5 >
	Unmethylated Forward	GGGGTTGGAATGTTTTGGGTTTGT	68 °C x 30
	Unmethylated Reverse	CAAACCTAAATCCCCACAAAACCA	72 °C x 5 >
<i>MOSCI</i>	Methylated Forward	TTAATGTAGTTTTAGTTCGAGGTTTTT CGTC	70 °C x 5 >
	Methylated Reverse	AAAAAAAAATACTACCAAACCTCCGC G	67 °C x 5 >
	Unmethylated Forward	TTGTTAATGTAGTTTTAGTTTGAGGTTT TTTGTT	64 °C x 30
	Unmethylated Reverse	AAAAAAAAATACTACCAAACCTCCAC ACC	70 °C x 5 >
<i>SNCG</i>	Methylated Forward	TAAGTTCGTAGTTCGTAGGGAGATTTA GTTTC	70 °C x 5 >
	Methylated Reverse	ATCTTTTCCACCGACCCACCACG	71 °C x 5 >
	Unmethylated Forward	GTTTAAGTTTGTAGTTTGTAGGGAGAT TTAGTTTTG	68 °C x 5 >
	Unmethylated Reverse	TAATCTTTTCCACCACCCACCACAC	65 °C x 30
<i>SOX11</i>	Methylated Forward	ATTATGGAGTAGTTTTTCGGATATGTAT AACGTC	74 °C x 5 >
	Methylated Reverse	TTATAATCGAAATAATCGACCATATAC TTAAACCG	71 °C x 5 >
	Unmethylated Forward	AAGATTATGGAGTAGTTTTTGGATATG TATAATGTT	68 °C x 5 >
	Unmethylated Reverse	ATACTTATAATCAAATAATCAACCAT ATACTTAAACCA	65 °C x 30
			70 °C x 5 >
			67 °C x 5 >
			64 °C x 30
			70 °C x 5 >
			67 °C x 5 >
			64 °C x 30

Supplementary Table 2b Pyrosequencing primers			
Gene Name	Primer	Primer Sequence (5' to 3')	T_{anneal} and cycles
<i>HNFI1A</i>	Forward	AGTTGGTTGAGTTGTTTAATG	57 °C x 55
	Reverse*	CCTCCTCAAAACTAAAATTCT	
	Sequencing	GGTTGAGTTGTTTAATG	
<i>HNFI1B</i>	Forward	GTAGTGTTTTTTTTTTGGATTAA	60 °C x 55
	Reverse*	CAAACCTCACCTAACCTTTAAA	
	Sequencing	GTAGTGTTTTTTTTTTGGAT	
<i>C14orf105</i>	Forward*	GTATTTATTTTTTTTAAAGGTAATTTAAG	59 °C x 55
	Reverse	CATACTAATTACCAAACTTTATTAATC	
	Sequencing	AAAAATTTATCCCCCA	
<i>KIF12</i>	Forward	GTAGAGTAGGATATGGAAGAA	60 °C x 55
	Reverse*	AATACCTCCTAACCAATTTATAC	
	Sequencing	TATTGTTGTTTATAGGGA	
<i>MIA2</i>	Forward	GATAGAAAAAGGTAGTTATTAAGAG	55 °C x 5 > 52 °C x 5 > 49 °C x 5 > 46 °C x 45
	Reverse*	CTCTCCAAACACTTTATCAA	
	Sequencing	TAAATTTTATTTGGGA	
<i>PAX8</i>	Forward*	GGGATAAGATTGGGATAG	52 °C x 55
	Reverse	CAAACCTCATCCTTTACAC	
	Sequencing	AACCTCATCCTTTACACC	
<i>SERPINA6</i>	Forward*	GATAAAGTTTTTTATTGGTTAATG	54 °C x 55
	Reverse	CCTAAACCCTAACATATATACA	
	Sequencing	CCTAAACCCTAACATATATACA	
<i>SGK2</i>	Forward	ATTAGGGAAGGTTGTGTAG	57 °C x 5 > 55 °C x 5 > 53 °C x 50
	Reverse*	CAACTCCCTAAACCTCATATAAA	
	Sequencing	TTAGTATTTAAGTTGGATTTTG	
<i>SRC</i>	Forward	GAATTTTTTGTGGTTATGTT	57 °C x 55
	Reverse*	ACAAAACCTTACTCTACACTAATCT	
	Sequencing	GAATTTTTTGTGGTTATG	
<i>TM4SF4</i>	Forward	GTTAGATTAAGGTGTAGTGG	60 °C x 5 > 57 °C x 5 > 54 °C x 5 > 51 °C x 45
	Reverse*	ATTTATACATTCTCCCTAACCC	

	Sequencing	GTGTTGGTGGATTATTAATAG	
<i>F2</i>	Forward	GGATTTGTTTTTTTAGATGGT	60 °C x 55
	Reverse*	CTCCCTTACCATACTAACTATAACAC	
	Sequencing	TTTTTAGATGGTGGAGA	
<i>ESR1</i>	Forward	GATGTTTAAGTTAATGTTAGGGTAAGGTAATAG	62 °C x 55
	Reverse*	AACCTCCAACCTTAAATACTAATCTC	
	Sequencing	ATGTTAGGGTAAGGTAATAG	
<i>BRCA1</i>	Forward	GTATTTTGAGAGGTTGTTGTTTAG	70 °C x 5 > 68 °C x 5 > 66 °C x 5 > 64 °C x 45
	Reverse*	AAAACCCCACAACCTATCC	
	Sequencing	TTTGAGAGGTTGTTGTTTA	
<i>IGF2</i>	Forward	GGAGGGGGTTTATTTTTTTAGGAAG	70 °C x 5 > 68 °C x 5 > 66 °C x 50
	Reverse*	AACCCCAACAAAACCACTAAACAC	
	Sequencing	GGGGTTTATTTTTTTAGGA	
* denotes biotinylated primer			

Supplementary Table 3 Differentially methylated genes between ovarian cancer cells and normal cells

	50 cell lines (genes)	93 clinical samples (genes)
Differentially methylated genes	2,003 / 14,495 (13.8%)	3,432 / 21,231 (16.2%)
Hypermethylated genes	1,870 (2,404 CpG sites)	2,383 (4,830 CpG sites)
Hypomethylated genes	139 (157 CpG sites)	1,253 (2,089 CpG sites)

Supplementary Table 4a Overlapping probes in cell lines and tissue specimens that are significantly hypermethylated in CCC.

Probe ID	Gene ID	Symbol	CPG ISLAND	Average beta value difference in cell lines	Average beta value difference in tissues	ER pathway
cg02104644	9066	SYT7	TRUE	0.2826	0.2220	
cg02927346	91608	RASL10B	TRUE	0.3962	0.2145	
cg03158400	54097	FAM3B	TRUE	0.3479	0.2041	
cg06339706	57664	PLEKHA4	FALSE	0.2617	0.2234	
cg07384961	9074	CLDN6	TRUE	0.2006	0.2439	
cg08725962	285598	ARL10	TRUE	0.4234	0.2791	
cg09715672	10974	C10orf116	TRUE	0.2884	0.2038	
cg09747578	10489	LRRC41	TRUE	0.2481	0.2070	
cg14377791	400696	LOC400696	FALSE	0.2789	0.2261	
cg14667273	64856	VWA1	TRUE	0.2345	0.2254	
cg17599586	23761	PISD	TRUE	0.3378	0.3007	
cg18702197	3232	HOXD3	TRUE	0.2456	0.2276	yes
cg18750960	3233	HOXD4	TRUE	0.3482	0.2292	yes
cg19257550	768	CA9	FALSE	0.3274	0.2628	
cg19718882	51352	WIT-1	TRUE	0.2721	0.2476	
cg20610181	768	CA9	FALSE	0.2151	0.2315	
cg21576698	7388	UQCRH	TRUE	0.4252	0.3183	
cg21949305	135	ADORA2A	FALSE	0.2369	0.2435	
cg22319147	1003	CDH5	FALSE	0.2063	0.2041	
cg22833027	8646	CHRD	TRUE	0.2201	0.2043	
cg23328404	55790	ChGn	FALSE	0.2344	0.2117	
cg24638647	84336	TMEM101	TRUE	0.5369	0.2012	
cg25228126	2535	FZD2	TRUE	0.2731	0.2384	
cg25229172	120935	CCDC38	TRUE	0.3337	0.2070	
cg27092035	285598	ARL10	TRUE	0.3797	0.2480	

Supplementary Table 4b Overlapping probes in cell lines and tissue specimens that are significantly hypomethylated in CCC.

Probe ID	Gene ID	Symbol	CPG ISLAND	Average beta value difference in cell lines	Average beta value difference in tissues	HNF1 pathway
cg11286122	23187	PHLDB1	FALSE	-0.3814	-0.2729	
cg11964613	415	ARSE	FALSE	-0.3942	-0.2249	
cg17463527	10110	SGK2	FALSE	-0.3234	-0.2119	yes
cg20199333	2147	F2	FALSE	-0.3332	-0.2182	yes
cg21495715	125206	SLC5A10	TRUE	-0.2791	-0.2637	
cg24747122	10672	GNA13	FALSE	-0.3507	-0.3057	

Supplementary Table 5a 276 genes (347 probes) identified as hypermethylated in CCC

Probe ID	Gene ID	Symbol	CPG ISLAND	U133A2	R value	P value
cg00186701	85453	TSPYL5	TRUE	213122 at	-0.6196	<0.0001
cg00236832	5914	RARA	FALSE	203749 s at	-0.3750	0.0144
cg00236832	5914	RARA	FALSE	211605 s at	-0.3625	0.0183
cg00236832	5914	RARA	FALSE	216300 x at	-0.3136	0.0431
cg00392257	81875	ISG20L2	FALSE	208114 s at	-0.4333	0.0042
cg00392257	81875	ISG20L2	FALSE	212766 s at	-0.3081	0.0471
cg00512374	3487	IGFBP4	TRUE	201508 at	-0.6309	<0.0001
cg00513220	54996	MOSC2	TRUE	221636 s at	-0.4610	0.0021
cg00513220	54996	MOSC2	TRUE	219527 at	-0.4163	0.0061
cg00564163	79689	STEAP4	TRUE	220187 at	-0.4924	0.0009
cg00655307	2099	ESR1	TRUE	205225 at	-0.3903	0.0106
cg00698688	6820	SULT2B1	FALSE	205759 s at	-0.5738	0.0001
cg00702231	5325	PLAGL1	TRUE	207002 s at	-0.6817	<0.0001
cg00702231	5325	PLAGL1	TRUE	207943 x at	-0.6774	<0.0001
cg00702231	5325	PLAGL1	TRUE	209318 x at	-0.6589	<0.0001
cg00725635	8707	B3GALT2	FALSE	210121 at	-0.3623	0.0184
cg00931491	6799	SULT1A2	FALSE	207122 x at	-0.4855	0.0011
cg00931491	6799	SULT1A2	FALSE	211385 x at	-0.4737	0.0015
cg00980978	10406	WFDC2	TRUE	203892 at	-0.5911	<0.0001
cg01062029	4920	ROR2	TRUE	205578 at	-0.4273	0.0048
cg01172484	28986	MAGEH1	TRUE	218573 at	-0.5489	0.0002
cg01240931	324	APC	FALSE	203525 s at	-0.4203	0.0056
cg01240931	324	APC	FALSE	203527 s at	-0.3801	0.0130
cg01240931	324	APC	FALSE	216933 x at	-0.3681	0.0165
cg01240931	324	APC	FALSE	203526 s at	-0.3633	0.0180
cg01283289	79611	FLJ21963	TRUE	219616 at	-0.6246	<0.0001
cg01318557	7462	LAT2	TRUE	221581 s at	-0.4849	0.0011
cg01420388	26232	FBXO2	TRUE	219305 x at	-0.6875	<0.0001
cg01593886	1277	COL1A1	TRUE	202310 s at	-0.4733	0.0015
cg01593886	1277	COL1A1	TRUE	217430 x at	-0.3982	0.0090
cg01593886	1277	COL1A1	TRUE	202311 s at	-0.3592	0.0195
cg01615704	7851	MALL	TRUE	209373 at	-0.5998	<0.0001
cg01657207	7584	ZNF35	FALSE	206096 at	-0.6963	<0.0001
cg01705587	9900	SV2A	TRUE	203069 at	-0.7719	<0.0001
cg01773854	3489	IGFBP6	TRUE	203851 at	-0.5245	0.0004
cg01795122	2014	EMP3	TRUE	203729 at	-0.7410	<0.0001
cg01805282	2070	EYA4	TRUE	207327 at	-0.4612	0.0021
cg02000005	1396	CRIP1	TRUE	205081 at	-0.7657	<0.0001
cg02175308	6272	SORT1	TRUE	212807 s at	-0.5740	0.0001
cg02175308	6272	SORT1	TRUE	212797 at	-0.5217	0.0004
cg02189785	9022	CLIC3	TRUE	219529 at	-0.6570	<0.0001
cg02257681	23564	DDAH2	TRUE	202262 x at	-0.6509	<0.0001
cg02257681	23564	DDAH2	TRUE	214909 s at	-0.6262	<0.0001
cg02257681	23564	DDAH2	TRUE	215537 x at	-0.6160	<0.0001
cg02265318	64757	MOSC1	TRUE	218865 at	-0.6016	<0.0001
cg02286990	79140	CCDC28B	TRUE	221912 s at	-0.5174	0.0004
cg02286990	79140	CCDC28B	TRUE	219585 at	-0.3952	0.0096
cg02497758	9935	MAFB	TRUE	218559 s at	-0.5279	0.0003
cg02508567	83439	TCF7L1	TRUE	221016 s at	-0.5883	<0.0001
cg02586730	30008	EFEMP2	TRUE	209356 x at	-0.8761	<0.0001
cg02586730	30008	EFEMP2	TRUE	206580 s at	-0.8589	<0.0001
cg02622316	9753	ZNF96	TRUE	217098 s at	-0.7006	<0.0001
cg02622316	9753	ZNF96	TRUE	206507 at	-0.5108	0.0005
cg02672493	80723	TMEM22	TRUE	219569 s at	-0.6431	<0.0001

cg02724472	10234	LRRC17	FALSE	205381	at	-0.4122	0.0067
cg02787991	6398	SECTM1	TRUE	213716	s at	-0.4677	0.0018
cg02833725	81875	ISG20L2	FALSE	208114	s at	-0.4060	0.0076
cg03000846	5881	RAC3	TRUE	206103	at	-0.5581	0.0001
cg03005261	55013	FLJ20647	TRUE	218802	at	-0.7221	<0.0001
cg03020951	3159	HMGA1	TRUE	210457	x at	-0.3971	0.0092
cg03020951	3159	HMGA1	TRUE	206074	s at	-0.3269	0.0346
cg03030757	2178	FANCE	TRUE	220255	at	-0.6148	<0.0001
cg03050522	9138	ARHGEF1	TRUE	203055	s at	-0.4528	0.0026
cg03070194	2946	GSTM2	FALSE	204418	x at	-0.5652	0.0001
cg03201604	27163	ASAH1	TRUE	214765	s at	-0.7533	<0.0001
cg03316864	10331	B3GNT3	TRUE	204856	at	-0.5613	0.0001
cg03365354	4162	MCAM	TRUE	210869	s at	-0.6013	<0.0001
cg03365354	4162	MCAM	TRUE	211340	s at	-0.5861	<0.0001
cg03365354	4162	MCAM	TRUE	209087	x at	-0.5720	0.0001
cg03365354	4162	MCAM	TRUE	209086	x at	-0.5045	0.0007
cg03557733	4355	MPP2	TRUE	207984	s at	-0.3071	0.0479
cg03568064	9479	MAPK8IP1	TRUE	213013	at	-0.4297	0.0045
cg03568064	9479	MAPK8IP1	TRUE	213014	at	-0.3374	0.0289
cg03614513	10100	TSPAN2	TRUE	214606	at	-0.4071	0.0075
cg03642357	157	ADRBK2	TRUE	204183	s at	-0.3548	0.0211
cg03642357	157	ADRBK2	TRUE	204184	s at	-0.3120	0.0442
cg03682712	4016	LOXL1	TRUE	203570	at	-0.7917	<0.0001
cg03691812	11151	CORO1A	TRUE	209083	at	-0.3862	0.0115
cg03705396	79929	MAP6D1	TRUE	221713	s at	-0.4775	0.0014
cg03718539	55224	ETNK2	TRUE	219268	at	-0.4728	0.0016
cg03740216	3386	ICAM4	TRUE	207194	s at	-0.3733	0.0149
cg03954173	976	CD97	FALSE	202910	s at	-0.7301	<0.0001
cg03985657	10712	C1orf2	TRUE	203550	s at	-0.6605	<0.0001
cg04273431	80742	PRR3	TRUE	204795	at	-0.3334	0.0309
cg04411625	1396	CRIP1	TRUE	205081	at	-0.6688	<0.0001
cg04444771	11067	C10orf10	FALSE	209183	s at	-0.4248	0.0050
cg04444771	11067	C10orf10	FALSE	209182	s at	-0.3277	0.0341
cg04544154	2000	ELF4	TRUE	203490	at	-0.4473	0.0030
cg04544154	2000	ELF4	TRUE	31845	at	-0.4315	0.0043
cg04676561	3009	HIST1H1B	TRUE	214534	at	-0.6048	<0.0001
cg04736140	23432	GPR161	TRUE	214104	at	-0.3356	0.0298
cg04736140	23432	GPR161	TRUE	206972	s at	-0.3149	0.0422
cg04743872	55022	FLJ20701	TRUE	219093	at	-0.5608	0.0001
cg04797323	8835	SOCS2	TRUE	203372	s at	-0.3437	0.0259
cg04797323	8835	SOCS2	TRUE	203373	at	-0.3059	0.0488
cg04809787	1140	CHRN1	TRUE	206703	at	-0.6730	<0.0001
cg04870470	2135	EXTL2	FALSE	209537	at	-0.5646	0.0001
cg04947157	11322	TMC6	TRUE	204328	at	-0.5990	<0.0001
cg04947157	11322	TMC6	TRUE	214958	s at	-0.5308	0.0003
cg05026186	22885	ABLIM3	TRUE	205730	s at	-0.4639	0.0020
cg05270634	8153	RND2	TRUE	213467	at	-0.6852	<0.0001
cg05361373	29108	PYCARD	TRUE	221666	s at	-0.9349	<0.0001
cg05600717	79758	FLJ13639	TRUE	204800	s at	-0.3800	0.0131
cg05659947	725	C4BPB	FALSE	208209	s at	-0.5477	0.0002
cg05677402	9246	UBE2L6	TRUE	201649	at	-0.6704	<0.0001
cg05932408	5740	PTGIS	TRUE	208131	s at	-0.3109	0.0451
cg06030619	11151	CORO1A	TRUE	209083	at	-0.4037	0.0080
cg06043114	10100	TSPAN2	TRUE	214606	at	-0.4301	0.0045
cg06100324	10232	MSLN	FALSE	204885	s at	-0.7830	<0.0001
cg06111454	4776	NFATC4	FALSE	213345	at	-0.3620	0.0185
cg06189653	80758	PRR7	TRUE	219742	at	-0.4099	0.0070
cg06191076	9077	DIRAS3	TRUE	215506	s at	-0.3519	0.0223
cg06207804	9048	ARTN	TRUE	207675	x at	-0.4670	0.0018
cg06207804	9048	ARTN	TRUE	216052	x at	-0.4214	0.0055
cg06207804	9048	ARTN	TRUE	210237	at	-0.4127	0.0066

cg06221259	51308	REEP2	TRUE	205331 s at	-0.6049	<0.0001
cg06311778	23371	TENC1	TRUE	212494 at	-0.4391	0.0036
cg06339706	57664	PLEKHA4	FALSE	219011 at	-0.3338	0.0307
cg06409153	23461	ABCA5	TRUE	213353 at	-0.5122	0.0005
cg06432655	25999	CLIPR-59	FALSE	212358 at	-0.7207	<0.0001
cg06791102	393	ARHGAP4	TRUE	204425 at	-0.8570	<0.0001
cg06885524	79901	CYBRD1	TRUE	217889 s at	-0.6701	<0.0001
cg06894812	4163	MCC	TRUE	206132 at	-0.4460	0.0031
cg06912252	84302	C9orf125	TRUE	213386 at	-0.5266	0.0003
cg07005513	9415	FADS2	TRUE	202218 s at	-0.5637	0.0001
cg07077459	5325	PLAGL1	TRUE	207002 s at	-0.6973	<0.0001
cg07077459	5325	PLAGL1	TRUE	207943 x at	-0.6927	<0.0001
cg07077459	5325	PLAGL1	TRUE	209318 x at	-0.6740	<0.0001
cg07112154	4355	MPP2	TRUE	207984 s at	-0.3466	0.0245
cg07112154	4355	MPP2	TRUE	213270 at	-0.3058	0.0489
cg07123069	3227	HOXC11	TRUE	206745 at	-0.7091	<0.0001
cg07138512	5909	RAP1GA1	TRUE	203911 at	-0.3206	0.0384
cg07200280	23180	RAFTLIN	TRUE	212646 at	-0.5676	0.0001
cg07211259	80380	PDCD1LG2	FALSE	220049 s at	-0.6064	<0.0001
cg07294541	50619	DEF6	TRUE	221293 s at	-0.5538	0.0001
cg07307078	84617	TUBB6	TRUE	209191 at	-0.3321	0.0316
cg07327468	2070	EYA4	TRUE	207327 at	-0.4436	0.0033
cg07328579	83468	GLT8D2	TRUE	221447 s at	-0.4901	0.0010
cg07384961	9074	CLDN6	TRUE	208474 at	-0.7665	<0.0001
cg07440414	6932	TCF7	TRUE	205255 x at	-0.4826	0.0012
cg07440414	6932	TCF7	TRUE	205254 x at	-0.4751	0.0015
cg07602200	5027	P2RX7	TRUE	207091 at	-0.4331	0.0042
cg07611334	80023	C20orf98	TRUE	218359 at	-0.7271	<0.0001
cg07640473	6405	SEMA3F	TRUE	206832 s at	-0.6499	<0.0001
cg07640473	6405	SEMA3F	TRUE	35666 at	-0.5823	0.0001
cg07640473	6405	SEMA3F	TRUE	209730 at	-0.4506	0.0027
cg07660236	9753	ZNF96	TRUE	217098 s at	-0.6258	<0.0001
cg07660236	9753	ZNF96	TRUE	206507 at	-0.4264	0.0049
cg07895149	51063	FAM26B	TRUE	57715 at	-0.7407	<0.0001
cg07895149	51063	FAM26B	TRUE	221565 s at	-0.7360	<0.0001
cg08052882	23530	NNT	FALSE	202784 s at	-0.7079	<0.0001
cg08052882	23530	NNT	FALSE	202783 at	-0.7076	<0.0001
cg08317263	26112	CCDC69	TRUE	212886 at	-0.3083	0.0470
cg08432727	6664	SOX11	TRUE	204914 s at	-0.5841	<0.0001
cg08432727	6664	SOX11	TRUE	204913 s at	-0.5496	0.0002
cg08432727	6664	SOX11	TRUE	204915 s at	-0.5084	0.0006
cg08441170	53904	MYO3A	TRUE	221400 at	-0.5064	0.0006
cg08496601	10682	EBP	TRUE	213787 s at	-0.7092	<0.0001
cg08496601	10682	EBP	TRUE	202735 at	-0.6932	<0.0001
cg08590939	5019	OXCT1	TRUE	202780 at	-0.6915	<0.0001
cg08629913	3489	IGFBP6	TRUE	203851 at	-0.5005	0.0007
cg08655844	81552	ECOP	TRUE	208091 s at	-0.3053	0.0493
cg08713365	80023	C20orf98	TRUE	218359 at	-0.7053	<0.0001
cg08955609	348	APOE	TRUE	203381 s at	-0.4138	0.0064
cg08955609	348	APOE	TRUE	212884 x at	-0.3521	0.0222
cg08955609	348	APOE	TRUE	203382 s at	-0.3339	0.0307
cg08965235	4054	LTBP3	TRUE	219922 s at	-0.6006	<0.0001
cg09001777	2525	FUT3	FALSE	214088 s at	-0.6803	<0.0001
cg09001777	2525	FUT3	FALSE	216010 x at	-0.6750	<0.0001
cg09208010	4323	MMP14	TRUE	202827 s at	-0.5983	<0.0001
cg09208010	4323	MMP14	TRUE	202828 s at	-0.5480	0.0002
cg09208010	4323	MMP14	TRUE	160020 at	-0.5321	0.0003
cg09208010	4323	MMP14	TRUE	217279 x at	-0.4454	0.0031
cg09243900	57111	RAB25	FALSE	218186 at	-0.9321	<0.0001
cg09405083	54838	C10orf26	FALSE	202808 at	-0.4065	0.0076
cg09580336	476	ATP1A1	TRUE	220948 s at	-0.4973	0.0008

cg09619786	54913	RPP25	TRUE	219143 s at	-0.6187	<0.0001
cg09715672	10974	C10orf116	TRUE	203571 s at	-0.8742	<0.0001
cg09747578	10489	LRRC41	TRUE	201932 at	-0.4973	0.0008
cg09747578	10489	LRRC41	TRUE	215765 at	-0.4163	0.0061
cg09786221	10398	MYL9	TRUE	201058 s at	-0.7382	<0.0001
cg09906488	57118	CAMK1D	TRUE	220246 at	-0.5089	0.0006
cg09998229	6915	TBXA2R	TRUE	336 at	-0.3615	0.0187
cg10084993	9351	SLC9A3R2	FALSE	209830 s at	-0.5323	0.0003
cg10107725	4065	LY75	TRUE	205668 at	-0.6306	<0.0001
cg10449070	217	ALDH2	TRUE	201425 at	-0.6293	<0.0001
cg10516359	55343	SLC35C1	TRUE	218485 s at	-0.3283	0.0338
cg10519140	2030	SLC29A1	TRUE	201802 at	-0.4493	0.0028
cg10519140	2030	SLC29A1	TRUE	201801 s at	-0.4144	0.0064
cg10520594	30833	NT5C	TRUE	219214 s at	-0.7350	<0.0001
cg10521852	9170	EDG4	TRUE	206722 s at	-0.6107	<0.0001
cg10521852	9170	EDG4	TRUE	206723 s at	-0.5801	0.0001
cg10541755	56648	EIF5A2	TRUE	220198 s at	-0.4680	0.0018
cg10557828	5352	PLOD2	TRUE	202619 s at	-0.5828	0.0001
cg10557828	5352	PLOD2	TRUE	202620 s at	-0.5665	0.0001
cg10564498	558	AXL	TRUE	202686 s at	-0.5775	0.0001
cg10564498	558	AXL	TRUE	202685 s at	-0.4485	0.0029
cg10599444	4323	MMP14	TRUE	202827 s at	-0.5723	0.0001
cg10599444	4323	MMP14	TRUE	202828 s at	-0.5311	0.0003
cg10599444	4323	MMP14	TRUE	160020 at	-0.5046	0.0007
cg10599444	4323	MMP14	TRUE	217279 x at	-0.4097	0.0071
cg10617171	6324	SCN1B	TRUE	205508 at	-0.3184	0.0399
cg10670077	3643	INSR	TRUE	213792 s at	-0.4016	0.0084
cg10682057	27163	ASAHL	TRUE	214765 s at	-0.6702	<0.0001
cg10731149	79901	CYBRD1	TRUE	217889 s at	-0.6959	<0.0001
cg10743104	10630	PDPN	TRUE	221898 at	-0.4221	0.0054
cg10743104	10630	PDPN	TRUE	204879 at	-0.3398	0.0277
cg10778619	27345	KCNMB4	TRUE	219287 at	-0.3531	0.0218
cg10857774	1760	DMPK	FALSE	37996 s at	-0.3411	0.0271
cg10857774	1760	DMPK	FALSE	217066 s at	-0.3270	0.0345
cg10983208	9806	SPOCK2	TRUE	202524 s at	-0.7936	<0.0001
cg10983208	9806	SPOCK2	TRUE	202523 s at	-0.7201	<0.0001
cg10995380	7041	TGFB111	TRUE	209651 at	-0.4626	0.0020
cg11059483	2100	ESR2	TRUE	211119 at	-0.4102	0.0070
cg11200929	1381	CRABP1	TRUE	205350 at	-0.3814	0.0127
cg11204562	79949	C10orf81	FALSE	219857 at	-0.3941	0.0098
cg11271605	79689	STEAP4	TRUE	220187 at	-0.3398	0.0277
cg11612291	7584	ZNF35	TRUE	206096 at	-0.7053	<0.0001
cg11745019	284	ANGPT1	TRUE	205608 s at	-0.3188	0.0396
cg11745019	284	ANGPT1	TRUE	205609 at	-0.3188	0.0396
cg11783497	3557	IL1RN	FALSE	212657 s at	-0.4367	0.0038
cg11783497	3557	IL1RN	FALSE	216243 s at	-0.4271	0.0048
cg11783497	3557	IL1RN	FALSE	212659 s at	-0.3860	0.0116
cg11840540	53827	FXYD5	TRUE	218084 x at	-0.3959	0.0095
cg11935147	9659	PDE4DIP	TRUE	210305 at	-0.3776	0.0137
cg11935147	9659	PDE4DIP	TRUE	209700 x at	-0.3556	0.0208
cg11970458	29108	PYCARD	TRUE	221666 s at	-0.8427	<0.0001
cg11976166	7042	TGFB2	TRUE	209909 s at	-0.6238	<0.0001
cg11976166	7042	TGFB2	TRUE	220407 s at	-0.6125	<0.0001
cg11976166	7042	TGFB2	TRUE	209908 s at	-0.5418	0.0002
cg12220493	7080	TITF1	TRUE	211024 s at	-0.4306	0.0044
cg12275348	8835	SOCS2	TRUE	203372 s at	-0.4114	0.0068
cg12275348	8835	SOCS2	TRUE	203373 at	-0.3803	0.0130
cg12412075	64130	LIN7B	TRUE	219760 at	-0.3146	0.0424
cg12438034	64110	MAGEF1	TRUE	218176 at	-0.4304	0.0044
cg12556134	60436	TGIF2	TRUE	218724 s at	-0.5367	0.0002
cg12556134	60436	TGIF2	TRUE	216262 s at	-0.5120	0.0005

cg12592716	8454	CUL1	TRUE	207614 s at	-0.3657	0.0173
cg12603043	30846	EHD2	TRUE	45297 at	-0.7284	<0.0001
cg12603043	30846	EHD2	TRUE	221870 at	-0.6951	<0.0001
cg12603043	30846	EHD2	TRUE	205341 at	-0.5009	0.0007
cg12621514	22943	DKK1	TRUE	204602 at	-0.5797	0.0001
cg12691219	51566	ARMCX3	TRUE	217858 s at	-0.7112	<0.0001
cg12757684	5325	PLAGL1	TRUE	207002 s at	-0.7103	<0.0001
cg12757684	5325	PLAGL1	TRUE	207943 x at	-0.7049	<0.0001
cg12757684	5325	PLAGL1	TRUE	209318 x at	-0.6886	<0.0001
cg12910797	3213	HOXB3	TRUE	208414 s at	-0.5578	0.0001
cg12970084	1999	ELF3	FALSE	201510 at	-0.4743	0.0015
cg12970084	1999	ELF3	FALSE	210827 s at	-0.3893	0.0108
cg12992720	9170	EDG4	TRUE	206722 s at	-0.7230	<0.0001
cg12992720	9170	EDG4	TRUE	206723 s at	-0.7106	<0.0001
cg13098960	6665	SOX15	FALSE	206122 at	-0.3849	0.0118
cg13302154	4256	MGP	FALSE	202291 s at	-0.3127	0.0438
cg13340269	59353	TMEM35	TRUE	219685 at	-0.5511	0.0002
cg13353683	284119	PTRF	TRUE	208789 at	-0.6925	<0.0001
cg13353683	284119	PTRF	TRUE	208790 s at	-0.6250	<0.0001
cg13376158	30833	NT5C	TRUE	219214 s at	-0.5930	<0.0001
cg13435381	8549	LGR5	TRUE	213880 at	-0.3697	0.0160
cg13496736	5017	OVOL1	TRUE	206604 at	-0.4072	0.0074
cg13523557	107	ADCY1	TRUE	213245 at	-0.3277	0.0341
cg13704271	79140	CCDC28B	TRUE	221912 s at	-0.5012	0.0007
cg13704271	79140	CCDC28B	TRUE	219585 at	-0.4241	0.0051
cg13828758	4692	NDN	TRUE	209550 at	-0.4724	0.0016
cg13877915	7691	ZNF132	TRUE	207402 at	-0.6607	<0.0001
cg13951472	11135	CDC42EP1	TRUE	204693 at	-0.6746	<0.0001
cg14030359	57447	NDRG2	TRUE	214279 s at	-0.5189	0.0004
cg14030359	57447	NDRG2	TRUE	206453 s at	-0.4174	0.0060
cg14070162	284119	PTRF	TRUE	208789 at	-0.7058	<0.0001
cg14070162	284119	PTRF	TRUE	208790 s at	-0.6457	<0.0001
cg14072120	5880	RAC2	TRUE	213603 s at	-0.7513	<0.0001
cg14072120	5880	RAC2	TRUE	207419 s at	-0.7024	<0.0001
cg14310034	652	BMP4	TRUE	211518 s at	-0.4575	0.0023
cg14417329	9123	SLC16A3	TRUE	202856 s at	-0.3656	0.0173
cg14417329	9123	SLC16A3	TRUE	202855 s at	-0.3630	0.0181
cg14435807	4016	LOXL1	TRUE	203570 at	-0.7842	<0.0001
cg14473924	23024	PDZRN3	TRUE	212915 at	-0.3727	0.0151
cg14564494	874	CBR3	FALSE	205379 at	-0.3551	0.0210
cg14566624	387509	GPR153	TRUE	221902 at	-0.3740	0.0147
cg14679587	27165	GLS2	TRUE	205531 s at	-0.5542	0.0001
cg14764661	9902	MRC2	FALSE	37408 at	-0.4973	0.0008
cg14833385	3108	HLA-DMA	FALSE	217478 s at	-0.5309	0.0003
cg14960043	50619	DEF6	TRUE	221293 s at	-0.5705	0.0001
cg15009813	8742	TNFSF12	FALSE	205611 at	-0.4258	0.0049
cg15014458	27076	LYPD3	FALSE	204952 at	-0.3457	0.0249
cg15020645	324	APC	FALSE	203525 s at	-0.3725	0.0151
cg15020645	324	APC	FALSE	203526 s at	-0.3080	0.0472
cg15227982	54838	C10orf26	FALSE	202808 at	-0.3647	0.0176
cg15247144	29108	PYCARD	TRUE	221666 s at	-0.9040	<0.0001
cg15309236	80823	BHLHB9	TRUE	213709 at	-0.6398	<0.0001
cg15379633	9609	RAB36	TRUE	211471 s at	-0.6632	<0.0001
cg15387123	9022	CLIC3	TRUE	219529 at	-0.7213	<0.0001
cg15426734	50855	PARD6A	TRUE	205245 at	-0.4379	0.0037
cg15526708	7046	TGFBR1	TRUE	206943 at	-0.3938	0.0099
cg15536490	7022	TFAP2C	TRUE	205286 at	-0.3369	0.0291
cg15536490	7022	TFAP2C	TRUE	205287 s at	-0.3259	0.0352
cg15640375	79948	PRG2	TRUE	220798 x at	-0.4070	0.0075
cg15684563	7103	TSPAN8	FALSE	203824 at	-0.5361	0.0003
cg15747595	85453	TSPYL5	TRUE	213122 at	-0.8511	<0.0001

cg15760840	3207	HOXA11	TRUE	208493 at	-0.4411	0.0035
cg15760840	3207	HOXA11	TRUE	213823 at	-0.4036	0.0080
cg15853125	7074	TIAM1	TRUE	213135 at	-0.3294	0.0331
cg15861540	6915	TBXA2R	TRUE	336 at	-0.3608	0.0189
cg16077929	8814	CDKL1	FALSE	207766 at	-0.4659	0.0019
cg16080552	4070	TACSTD2	TRUE	202286 s at	-0.8576	<0.0001
cg16080552	4070	TACSTD2	TRUE	202287 s at	-0.3967	0.0093
cg16092786	7490	WT1	TRUE	216953 s at	-0.3714	0.0155
cg16227684	2664	GDI1	TRUE	201864 at	-0.3349	0.0302
cg16500334	6612	SUMO3	TRUE	200739 s at	-0.5857	<0.0001
cg16500334	6612	SUMO3	TRUE	200740 s at	-0.5796	0.0001
cg16786703	101	ADAM8	TRUE	205179 s at	-0.4750	0.0015
cg16786703	101	ADAM8	TRUE	205180 s at	-0.4283	0.0047
cg16792632	2100	ESR2	TRUE	211119 at	-0.3629	0.0182
cg16914151	54913	RPP25	TRUE	219143 s at	-0.5218	0.0004
cg16970232	324	APC	TRUE	203525 s at	-0.3487	0.0236
cg17114257	9873	FCHSD2	TRUE	203620 s at	-0.3090	0.0465
cg17285325	1890	ECGF1	TRUE	217497 at	-0.3395	0.0278
cg17285325	1890	ECGF1	TRUE	204858 s at	-0.3271	0.0345
cg17441778	4647	MYO7A	TRUE	33197 at	-0.3315	0.0320
cg17470697	219654	C10orf56	TRUE	212423 at	-0.3648	0.0175
cg17501569	10232	MSLN	TRUE	204885 s at	-0.8413	<0.0001
cg17503456	668	FOXL2	TRUE	220102 at	-0.5848	<0.0001
cg17550582	81031	SLC2A10	TRUE	221024 s at	-0.6575	<0.0001
cg17682828	53822	FXYD7	TRUE	220131 at	-0.3210	0.0382
cg17691309	7169	TPM2	TRUE	204083 s at	-0.7812	<0.0001
cg17691309	7169	TPM2	TRUE	212654 at	-0.5821	0.0001
cg17787710	5881	RAC3	TRUE	206103 at	-0.4671	0.0018
cg17800442	1489	CTF1	TRUE	206813 at	-0.4524	0.0026
cg17805404	27239	GPR162	FALSE	205056 s at	-0.6196	<0.0001
cg17980508	10964	IFI44L	FALSE	204439 at	-0.3572	0.0202
cg18265887	5880	RAC2	TRUE	213603 s at	-0.7971	<0.0001
cg18265887	5880	RAC2	TRUE	207419 s at	-0.7499	<0.0001
cg18273501	51063	FAM26B	TRUE	221565 s at	-0.7453	<0.0001
cg18273501	51063	FAM26B	TRUE	57715 at	-0.7400	<0.0001
cg18702197	3232	HOXD3	TRUE	206602 s at	-0.4175	0.0059
cg18702197	3232	HOXD3	TRUE	206601 s at	-0.3835	0.0122
cg18727700	27286	SRPX2	FALSE	205499 at	-0.5674	0.0001
cg18750960	3233	HOXD4	TRUE	205522 at	-0.5424	0.0002
cg18884137	1140	CHRNB1	TRUE	206703 at	-0.6573	<0.0001
cg18937321	6536	SLC6A9	TRUE	207043 s at	-0.5411	0.0002
cg18950617	23526	HMHA1	TRUE	212873 at	-0.3081	0.0471
cg19008649	3488	IGFBP5	TRUE	211959 at	-0.3880	0.0111
cg19038540	1901	EDG1	TRUE	204642 at	-0.3515	0.0225
cg19055639	9823	ARMCX2	TRUE	203404 at	-0.6104	<0.0001
cg19186356	217	ALDH2	TRUE	201425 at	-0.4215	0.0054
cg19257550	768	CA9	FALSE	205199 at	-0.5935	<0.0001
cg19481953	27286	SRPX2	FALSE	205499 at	-0.5532	0.0001
cg19514469	79767	ELMO3	TRUE	219411 at	-0.8847	<0.0001
cg19614321	9770	RASSF2	FALSE	203185 at	-0.3217	0.0378
cg19713460	9145	SYNGR1	TRUE	210613 s at	-0.5852	<0.0001
cg19713460	9145	SYNGR1	TRUE	213854 at	-0.5836	<0.0001
cg19713460	9145	SYNGR1	TRUE	204287 at	-0.5521	0.0002
cg19744952	23152	CIC	TRUE	212784 at	-0.3075	0.0476
cg19764436	2781	GNAZ	TRUE	204993 at	-0.5165	0.0005
cg19786920	79730	FLJ14001	TRUE	220194 at	-0.4819	0.0012
cg19826026	397	ARHGDIB	FALSE	201288 at	-0.5869	<0.0001
cg19928046	972	CD74	FALSE	209619 at	-0.7322	<0.0001
cg20008332	6664	SOX11	TRUE	204914 s at	-0.6606	<0.0001
cg20008332	6664	SOX11	TRUE	204913 s at	-0.6491	<0.0001
cg20008332	6664	SOX11	TRUE	204915 s at	-0.5964	<0.0001

cg20311501	324	APC	TRUE	203525 s at	-0.3434	0.0260
cg20330472	2070	EYA4	TRUE	207327 at	-0.3901	0.0107
cg20442697	10234	LRRC17	FALSE	205381 at	-0.3918	0.0103
cg20484352	92689	LOC92689	TRUE	213455 at	-0.6970	<0.0001
cg20610181	768	CA9	FALSE	205199 at	-0.5657	0.0001
cg20627916	2099	ESR1	TRUE	205225 at	-0.5442	0.0002
cg20627916	2099	ESR1	TRUE	215552 s at	-0.4419	0.0034
cg20627916	2099	ESR1	TRUE	217190 x at	-0.3686	0.0163
cg20718816	4053	LTBP2	TRUE	204682 at	-0.4225	0.0053
cg20775959	9915	ARNT2	TRUE	202986 at	-0.6756	<0.0001
cg20786074	2202	EFEMP1	TRUE	201843 s at	-0.4575	0.0023
cg20786074	2202	EFEMP1	TRUE	201842 s at	-0.4339	0.0041
cg20877313	27165	GLS2	TRUE	205531 s at	-0.5435	0.0002
cg20908204	1760	DMPK	FALSE	37996 s at	-0.3669	0.0168
cg20909686	5017	OVOL1	TRUE	206604 at	-0.4542	0.0025
cg20947775	79966	SCD5	TRUE	220232 at	-0.3143	0.0426
cg21012874	6623	SNCG	TRUE	209877 at	-0.6944	<0.0001
cg21034676	7045	TGFBI	TRUE	201506 at	-0.4340	0.0041
cg21279955	11000	SLC27A3	TRUE	222217 s at	-0.6732	<0.0001
cg21522303	10610	ST6GALNAC2	TRUE	204542 at	-0.5872	<0.0001
cg21572316	19	ABCA1	TRUE	203504 s at	-0.5591	0.0001
cg21572316	19	ABCA1	TRUE	203505 at	-0.5472	0.0002
cg21572316	19	ABCA1	TRUE	216066 at	-0.3344	0.0304
cg21576698	7388	UQCRH	TRUE	202233 s at	-0.8685	<0.0001
cg21634602	324	APC	TRUE	203525 s at	-0.3404	0.0274
cg21671476	10398	MYL9	TRUE	201058 s at	-0.8149	<0.0001
cg21838334	10763	NES	TRUE	218678 at	-0.3372	0.0290
cg22130834	55001	TTC22	TRUE	215106 at	-0.4373	0.0038
cg22130834	55001	TTC22	TRUE	215107 s at	-0.4319	0.0043
cg22130834	55001	TTC22	TRUE	220309 at	-0.3256	0.0354
cg22238923	1796	DOK1	TRUE	211121 s at	-0.4750	0.0015
cg22238923	1796	DOK1	TRUE	216835 s at	-0.4394	0.0036
cg22319147	1003	CDH5	FALSE	204677 at	-0.6389	<0.0001
cg22343001	9823	ARMCX2	TRUE	203404 at	-0.8057	<0.0001
cg22392276	1152	CKB	TRUE	200884 at	-0.3230	0.0370
cg22392708	25984	KRT23	FALSE	218963 s at	-0.4507	0.0027
cg22467567	3488	IGFBP5	TRUE	211959 at	-0.4891	0.0010
cg22467567	3488	IGFBP5	TRUE	211958 at	-0.4200	0.0056
cg22467567	3488	IGFBP5	TRUE	203425 s at	-0.3798	0.0131
cg22467567	3488	IGFBP5	TRUE	203424 s at	-0.3691	0.0162
cg22633722	875	CBS	TRUE	212816 s at	-0.4280	0.0047
cg22731373	9468	PCYT1B	FALSE	206751 s at	-0.3259	0.0352
cg22780475	23624	CBLC	TRUE	220638 s at	-0.8473	<0.0001
cg22874046	3383	ICAM1	TRUE	202638 s at	-0.4388	0.0037
cg22874046	3383	ICAM1	TRUE	202637 s at	-0.3828	0.0123
cg22930187	9048	ARTN	TRUE	207675 x at	-0.3837	0.0121
cg22930187	9048	ARTN	TRUE	216052 x at	-0.3551	0.0210
cg22930187	9048	ARTN	TRUE	210237 at	-0.3211	0.0382
cg22939715	10712	C1orf2	TRUE	203550 s at	-0.6279	<0.0001
cg22968401	51268	PIPOX	FALSE	221605 s at	-0.3921	0.0102
cg22975913	7490	WT1	TRUE	216953 s at	-0.3452	0.0252
cg23165541	23604	DAPK2	TRUE	206324 s at	-0.4154	0.0062
cg23263923	970	TNFSF7	TRUE	206508 at	-0.4852	0.0011
cg23337754	1381	CRABP1	TRUE	205350 at	-0.3079	0.0473
cg23412850	8835	SOCS2	TRUE	203372 s at	-0.3346	0.0303
cg23412850	8835	SOCS2	TRUE	203373 at	-0.3059	0.0488
cg23452458	114881	OSBPL7	FALSE	210344 at	-0.3634	0.0180
cg23452458	114881	OSBPL7	FALSE	208163 s at	-0.3287	0.0336
cg23710218	9242	MSC	TRUE	209928 s at	-0.3841	0.0120
cg23771603	53904	MYO3A	TRUE	221400 at	-0.5112	0.0005
cg23771661	10331	B3GNT3	TRUE	204856 at	-0.3138	0.0430

cg23887396	23098	SARM1	TRUE	213259 s at	-0.6578	<0.0001
cg23887396	23098	SARM1	TRUE	213257 at	-0.5604	0.0001
cg24070292	7169	TPM2	TRUE	204083 s at	-0.8335	<0.0001
cg24070292	7169	TPM2	TRUE	212654 at	-0.7090	<0.0001
cg24130010	140578	CHODL	TRUE	219867 at	-0.4763	0.0014
cg24155668	5603	MAPK13	TRUE	210059 s at	-0.8278	<0.0001
cg24155668	5603	MAPK13	TRUE	210058 at	-0.8210	<0.0001
cg24332422	324	APC	TRUE	203525 s at	-0.3625	0.0183
cg24384676	89874	SLC25A21	TRUE	220474 at	-0.3545	0.0213
cg24447042	6594	SMARCA1	TRUE	203875 at	-0.3948	0.0097
cg24447042	6594	SMARCA1	TRUE	215294 s at	-0.3619	0.0185
cg24447042	6594	SMARCA1	TRUE	203874 s at	-0.3556	0.0208
cg24594997	5947	RBP1	TRUE	203423 at	-0.6506	<0.0001
cg24794531	7220	TRPC1	TRUE	205803 s at	-0.4130	0.0066
cg24794531	7220	TRPC1	TRUE	205802 at	-0.3323	0.0315
cg24794531	7220	TRPC1	TRUE	211602 s at	-0.3227	0.0371
cg24852661	51280	GOLPH2	TRUE	217771 at	-0.4894	0.0010
cg24860534	8476	CDC42BPA	TRUE	214464 at	-0.4000	0.0087
cg24860534	8476	CDC42BPA	TRUE	213595 s at	-0.3197	0.0390
cg24930915	25837	RAB26	TRUE	219562 at	-0.4267	0.0048
cg24930915	25837	RAB26	TRUE	50965 at	-0.4033	0.0081
cg25228126	2535	FZD2	TRUE	210220 at	-0.3563	0.0206
cg25300386	1278	COL1A2	TRUE	202403 s at	-0.4685	0.0018
cg25300386	1278	COL1A2	TRUE	202404 s at	-0.4097	0.0071
cg25341653	79767	ELMO3	TRUE	219411 at	-0.8910	<0.0001
cg25361106	3196	TLX2	TRUE	211049 at	-0.3396	0.0278
cg25416372	53637	EDG8	TRUE	221417 x at	-0.3412	0.0270
cg25589890	80329	ULBP1	TRUE	221323 at	-0.3051	0.0494
cg25799986	10406	WFDC2	TRUE	203892 at	-0.6934	<0.0001
cg25821963	22885	ABLIM3	TRUE	205730 s at	-0.3307	0.0324
cg25836271	10235	RASGRP2	TRUE	208206 s at	-0.3446	0.0254
cg25946374	58985	IL22RA1	FALSE	220056 at	-0.4593	0.0022
cg26014796	80352	RNF39	TRUE	219916 s at	-0.3787	0.0134
cg26036443	30846	EHD2	TRUE	45297 at	-0.7666	<0.0001
cg26036443	30846	EHD2	TRUE	221870 at	-0.7187	<0.0001
cg26036443	30846	EHD2	TRUE	205341 at	-0.5997	<0.0001
cg26117023	1796	DOK1	TRUE	211121 s at	-0.6908	<0.0001
cg26117023	1796	DOK1	TRUE	216835 s at	-0.6623	<0.0001
cg26220350	5360	PLTP	TRUE	202075 s at	-0.6995	<0.0001
cg26279025	3589	IL11	TRUE	206924 at	-0.3899	0.0107
cg26317056	23530	NNT	TRUE	202783 at	-0.6896	<0.0001
cg26317056	23530	NNT	TRUE	202784 s at	-0.6736	<0.0001
cg26333317	25840	METTL7A	FALSE	207761 s at	-0.4685	0.0018
cg26333317	25840	METTL7A	FALSE	209703 x at	-0.3325	0.0314
cg26968812	7171	TPM4	TRUE	212481 s at	-0.6165	<0.0001
cg26968812	7171	TPM4	TRUE	209344 at	-0.6092	<0.0001
cg26987645	2331	FMOD	TRUE	202709 at	-0.4221	0.0054
cg27176536	25837	RAB26	TRUE	219562 at	-0.4269	0.0048
cg27176536	25837	RAB26	TRUE	50965 at	-0.3894	0.0108
cg27234090	9099	USP2	TRUE	207213 s at	-0.3284	0.0337
cg27264345	51308	REEP2	TRUE	205331 s at	-0.4892	0.0010
cg27329371	218	ALDH3A1	FALSE	205623 at	-0.3191	0.0394
cg27379587	4828	NMB	TRUE	205204 at	-0.6882	<0.0001
cg27397287	976	CD97	TRUE	202910 s at	-0.6930	<0.0001
cg27420236	56475	RPRM	TRUE	219370 at	-0.4385	0.0037

Supplementary Table 5b 22 genes (30 probes) identified as hypomethylated in CCC

Probe ID	Gene ID	Symbol	CPG ISLAND	U133A2	R value	P value
cg02286642	9534	ZNF254	FALSE	206862 at	-0.3218	0.0377
cg02335804	6928	TCF2	FALSE	205313 at	-0.7712	<0.0001
cg02335804	6928	TCF2	FALSE	208135 at	-0.5324	0.0003
cg06444781	6927	TCF1	TRUE	210515 at	-0.4036	0.0080
cg07403255	7849	PAX8	TRUE	214528 s at	-0.8830	<0.0001
cg07403255	7849	PAX8	TRUE	209552 at	-0.8549	<0.0001
cg07403255	7849	PAX8	TRUE	121 at	-0.8494	<0.0001
cg07403255	7849	PAX8	TRUE	207924 x at	-0.8485	<0.0001
cg07403255	7849	PAX8	TRUE	207923 x at	-0.8207	<0.0001
cg07403255	7849	PAX8	TRUE	213917 at	-0.7862	<0.0001
cg07403255	7849	PAX8	TRUE	207921 x at	-0.7845	<0.0001
cg07403255	7849	PAX8	TRUE	221990 at	-0.6610	<0.0001
cg07810156	10158	PDZK1IP1	FALSE	219630 at	-0.8312	<0.0001
cg10025865	866	SERPINA6	FALSE	206325 at	-0.4837	0.0012
cg10321723	5174	PDZK1	FALSE	205380 at	-0.5911	<0.0001
cg10734665	57194	ATP10A	TRUE	214255 at	-0.7310	<0.0001
cg11286122	23187	PHLDB1	FALSE	212134 at	-0.3343	0.0305
cg11639651	80201	HKDC1	FALSE	220585 at	-0.5194	0.0004
cg11762346	80201	HKDC1	FALSE	220585 at	-0.6174	<0.0001
cg11964613	415	ARSE	FALSE	205894 at	-0.6941	<0.0001
cg12640109	80150	ASRGL1	TRUE	218857 s at	-0.4588	0.0022
cg12762799	26253	CLEC4E	FALSE	219859 at	-0.4962	0.0008
cg12788467	6928	TCF2	TRUE	205313 at	-0.8305	<0.0001
cg12788467	6928	TCF2	TRUE	208135 at	-0.5391	0.0002
cg13019092	5174	PDZK1	FALSE	205380 at	-0.5092	0.0006
cg13652336	80243	DEPDC2	TRUE	220732 at	-0.4743	0.0015
cg13688966	7104	TM4SF4	FALSE	209937 at	-0.4877	0.0011
cg15187606	10158	PDZK1IP1	FALSE	219630 at	-0.4569	0.0024
cg15661409	55195	C14orf105	FALSE	220084 at	-0.6212	<0.0001
cg15967525	54502	FLJ20273	FALSE	218035 s at	-0.4271	0.0048
cg16175725	6927	TCF1	TRUE	210515 at	-0.4792	0.0013
cg17463527	10110	SGK2	FALSE	220357 s at	-0.6872	<0.0001
cg20199333	2147	F2	FALSE	205754 at	-0.7240	<0.0001
cg21516287	65999	LRRC61	TRUE	218907 s at	-0.6681	<0.0001
cg21685427	10110	SGK2	FALSE	220357 s at	-0.6172	<0.0001
cg22376897	415	ARSE	FALSE	205894 at	-0.5956	<0.0001
cg24248317	54978	C2orf18	TRUE	219783 at	-0.6582	<0.0001
cg24603941	117153	MIA2	FALSE	221177 at	-0.6689	<0.0001
cg25042226	7849	PAX8	TRUE	214528 s at	-0.8888	<0.0001
cg25042226	7849	PAX8	TRUE	209552 at	-0.8627	<0.0001
cg25042226	7849	PAX8	TRUE	207924 x at	-0.8585	<0.0001
cg25042226	7849	PAX8	TRUE	121 at	-0.8569	<0.0001
cg25042226	7849	PAX8	TRUE	207923 x at	-0.8282	<0.0001
cg25042226	7849	PAX8	TRUE	207921 x at	-0.7884	<0.0001
cg25042226	7849	PAX8	TRUE	213917 at	-0.7836	<0.0001
cg25042226	7849	PAX8	TRUE	221990 at	-0.6686	<0.0001

Supplementary Table 6 Categorical analysis of ‘transcription factor targets’ of 22 UM genes in CCC ^a			
MSigID.c3.tft	probes	z score	p value
V\$HNF1_Q6*	340	13.91	<0.000001
V\$PPARA_01	47	10.88	<0.000001
V\$HNF6_Q6	301	8.29	<0.000001
V\$HNF1_C*	304	8.24	<0.000001
V\$HNF1_01*	305	8.23	<0.000001
RGTTAMWNATT_V\$HNF1_01*	99	7.36	<0.000001
V\$SER_Q6_01	317	5.92	<0.000001
V\$TEF_Q6	326	5.83	<0.000001
V\$HNF4_01	347	5.62	<0.000001
V\$NKX25_01	169	5.49	<0.000001
V\$CDPCR1_01	180	5.30	<0.000001
RAAGNYNNCTTY_UNKNOWN	181	5.28	<0.000001
V\$FOXD3_01	278	4.11	1.99E-05
V\$AR_Q6	279	4.10	2.07E-05

a All four terms representing HNF1 transcription factor binding activity (*) were enriched among the 22 CCC-specific UM genes.

Supplementary Figure Legends

Supplementary Figure 1 Scheme of methodologies used for (A) the identification of genes exhibiting differential methylation between CCC and non-CCC cells and (B) the identification of candidate genes functionally regulated by DNA methylation in CCC.

Supplementary Figure 2 Validation of Infinium beta-values by quantitative bisulfite pyrosequencing of the same CpG site represented on the Infinium platform.

Supplementary Figure 3 Correlation between the Infinium assay beta-values and methylation values as measured by quantitative bisulfite pyrosequencing for CpG sites adjacent to those represented on the Infinium platform.

Supplementary Figure 4 Supervised hierarchical clustering of two independent expression microarray datasets using clinical samples, GSE6008 (A) and GSE2109 (B), was performed using only the genes regulated by DNA methylation listed in Supplementary Table 5. CCC was clearly divided from non-CCC samples by these genes. The CCC-specific UM genes generated a distinct cluster of genes highly expressed in CCC (yellow squares). The color bar on the right represents methylation status; red indicates CCC-specific UM genes and green indicates CCC-specific HM genes.

Supplementary Figure 5 Amplicons produced from cell lines by methylation-specific PCR for six ERalpha network genes: *ESR1* (A), *BMP4* (B), *DKK1* (C), *SOX11* (D), *SNCG* (E) and *MOSCI* (F). Some samples were analyzed in duplicate. Abbreviations; M: amplicons produced from the primer set complementary to the methylated bisulfite modified sequence, U: amplicons produced from the primer set complementary to the unmethylated bisulfite modified sequence, (+): bisulfite modified CpGenome Universal Methylated DNA (Millipore Co.) as positive control, g: genomic DNA, 0%: human normal lymphocytes, 50%: a 50:50 mixture of positive control and normal lymphocytes, 100%: positive methylated control, NTC: no template control.

Supplementary Figure 6 Amplicons produced from clinical ovarian cancer specimens by methylation-specific PCR for six ERalpha network genes: *ESR1* (A), *BMP4* (B), *DKK1* (C), *SOX11* (D), *SNCG* (E) and *MOSCI* (F). Some samples were analyzed in duplicate. Abbreviations; M: amplicons produced from the primer set complementary to the methylated bisulfite modified sequence, U: amplicons produced from the primer set complementary to the unmethylated bisulfite modified sequence, (+): bisulfite modified CpGenome Universal Methylated DNA (Millipore Co.) as positive control, g: genomic DNA, 0%: human normal lymphocytes, 50%: a 50:50 mixture of positive control and normal lymphocytes, 100%: positive methylated control, NTC: no template control.

Supplementary Figure 1

a)



1. Student t-tests $p < 0.01$
2. Average beta value difference > 0.2

Hypomethylation in CCC
44 genes (54 CpG sites)

Hypermethylation in CCC
856 genes (1042 CpG sites)

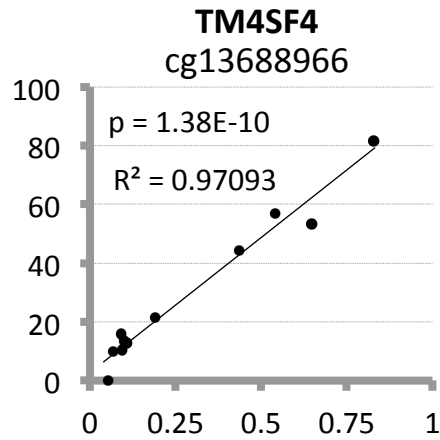
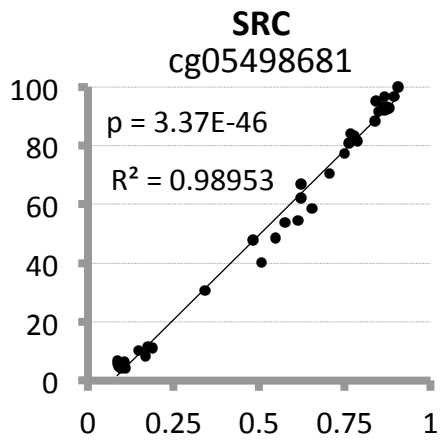
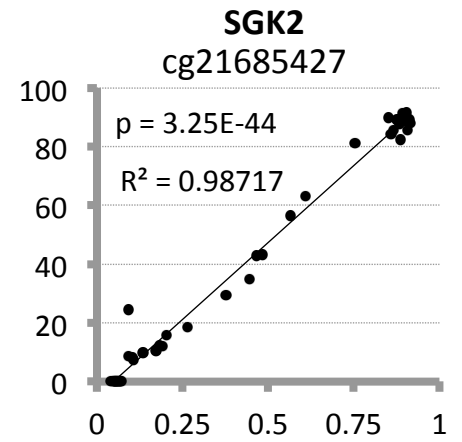
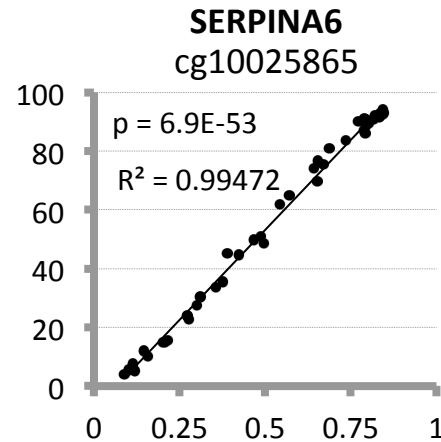
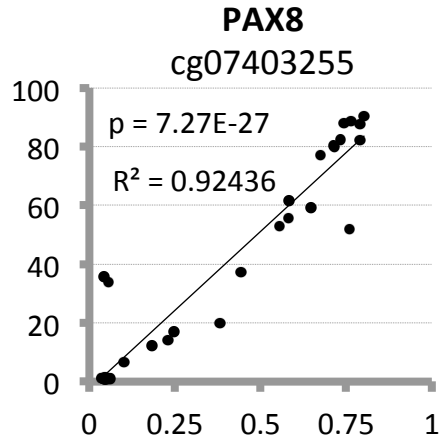
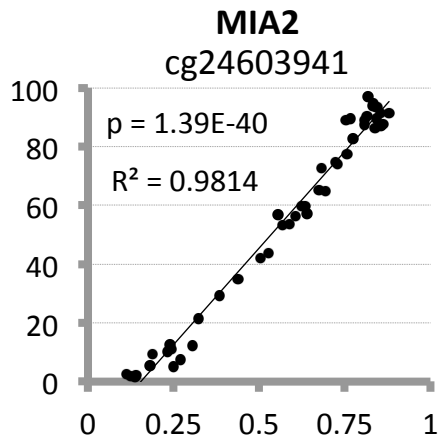
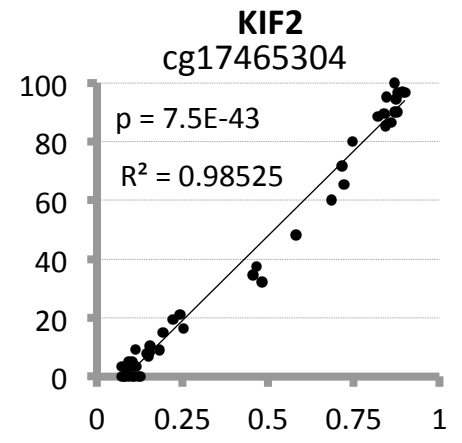
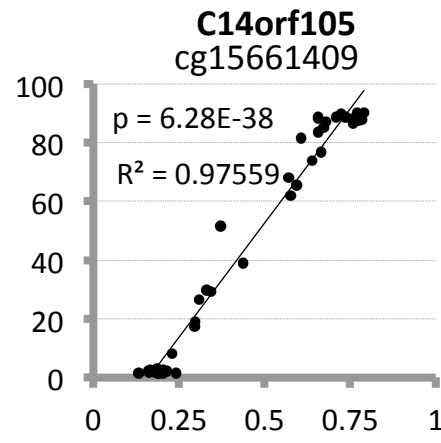
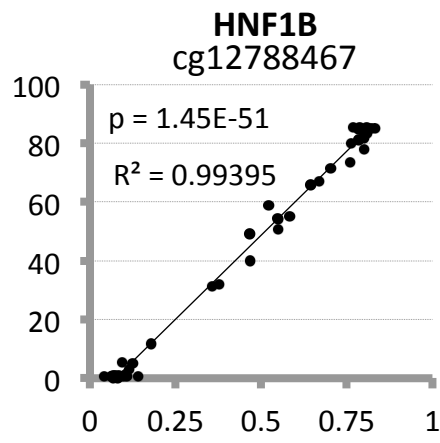
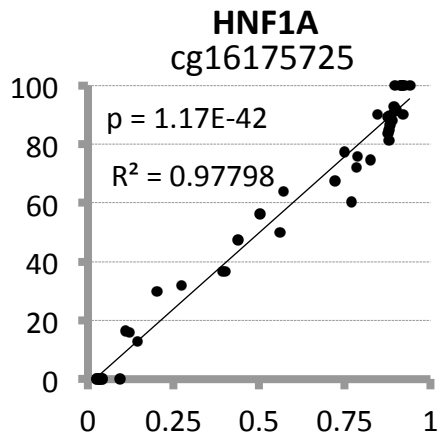
b)

3. Inverse correlation between beta-value and mRNA expression in 42 ovarian cancer parental cell lines ($p < 0.05$)

Activated via hypomethylation in CCC
22 genes / total 33 genes (66.7%)

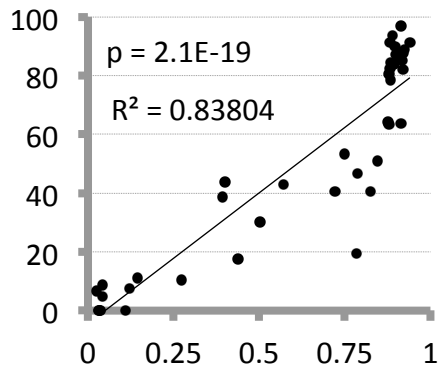
Suppressed via hypermethylation in CCC
276 genes / total 625 genes (44.2%)

Supplementary Figure 2

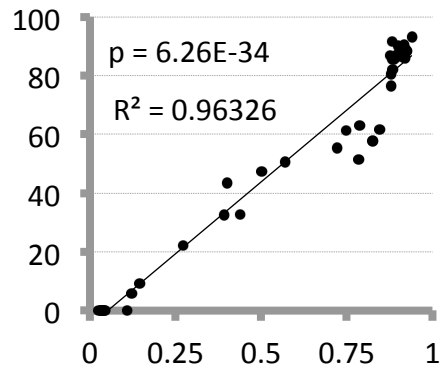


Supplementary Figure 3

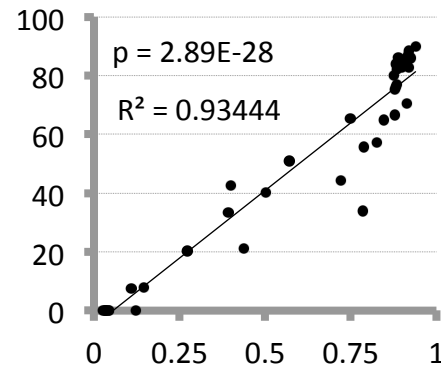
HNF1A_Pos.1



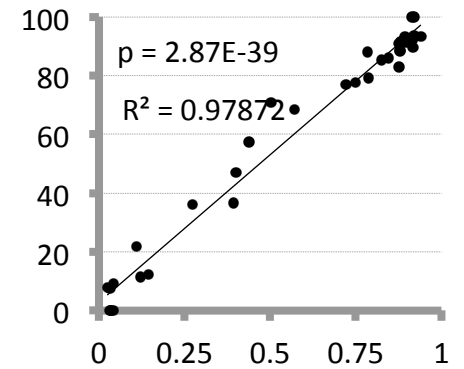
HNF1A_Pos.2



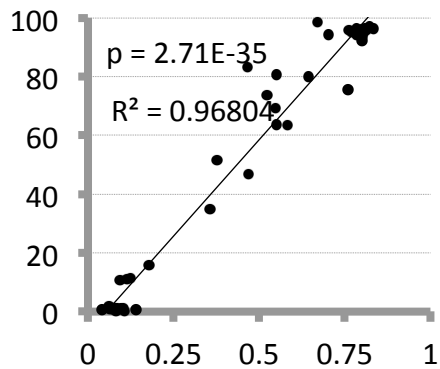
HNF1A_Pos.3



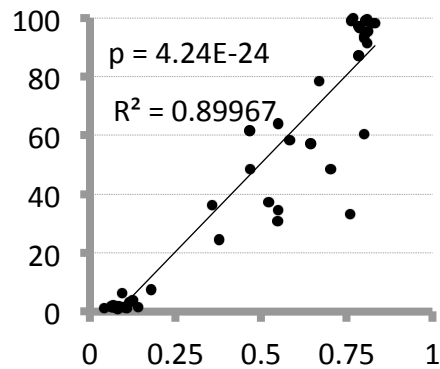
HNF1A_Pos.4



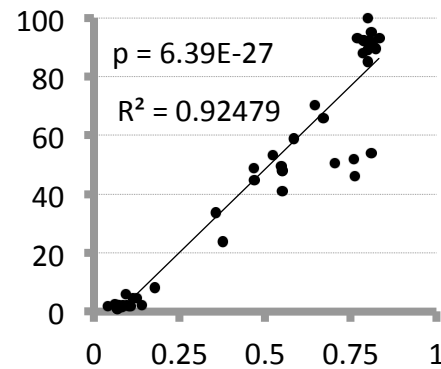
HNF1B_Pos.1



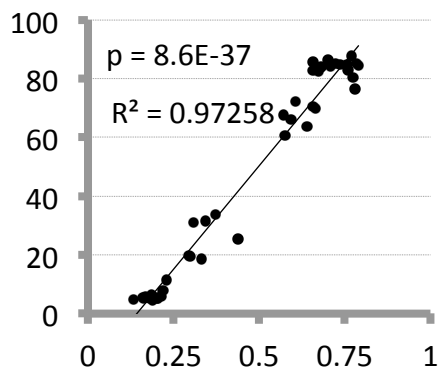
HNF1B_Pos.2



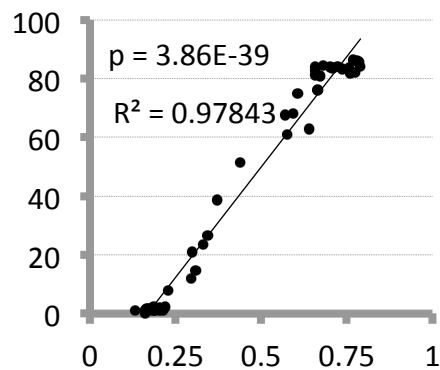
HNF1B_Pos.3



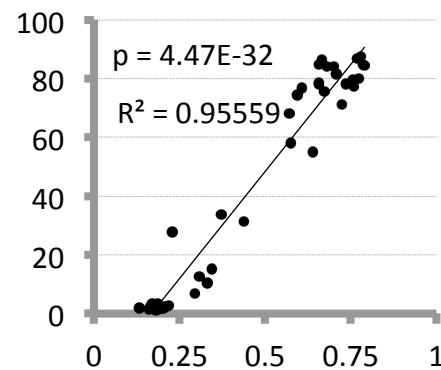
C14orf105_Pos.1



C14orf105_Pos.3

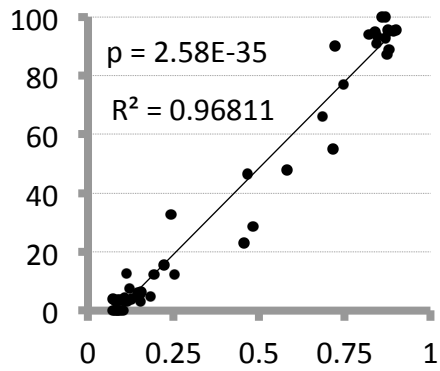


C14orf105_Pos.4

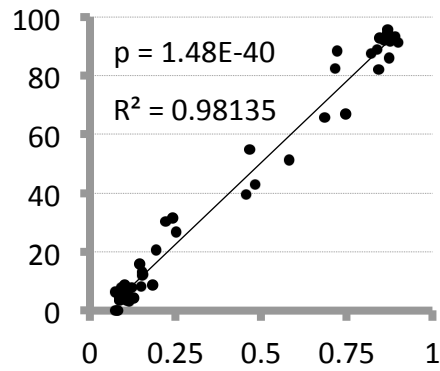


Supplementary Figure 3 (cont.)

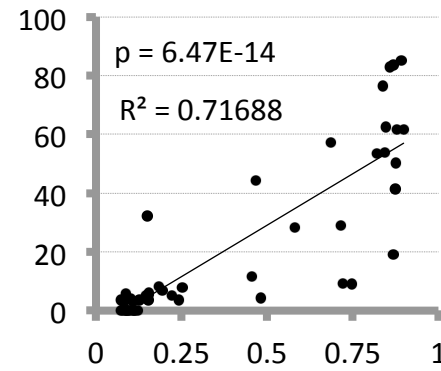
KIF12_Pos.2



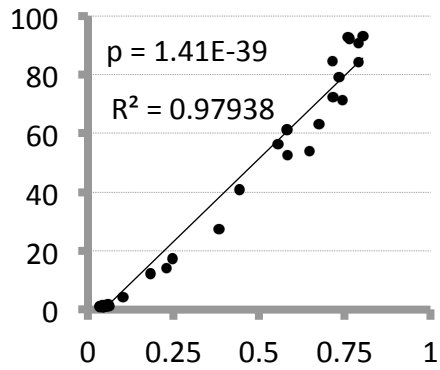
KIF12_Pos.3



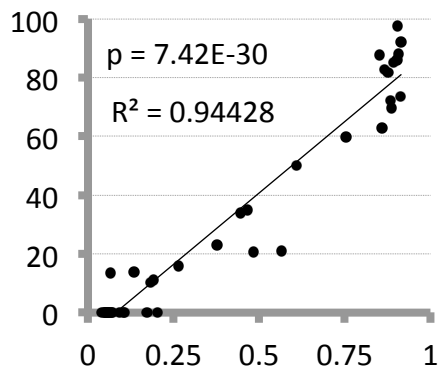
KIF12_Pos.4



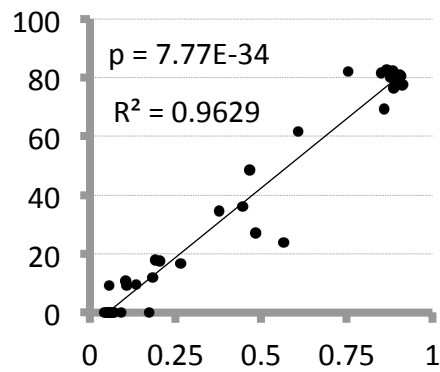
PAX8_Pos.1



SGK2_Pos.2

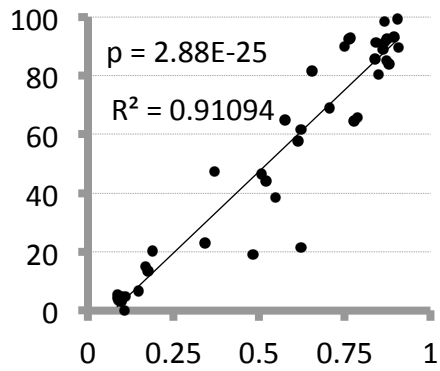


SGK2_Pos.3

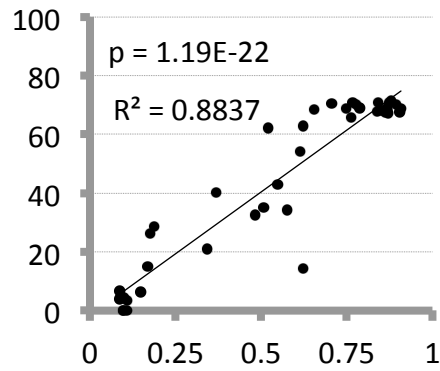


Supplementary Figure 3 (cont.)

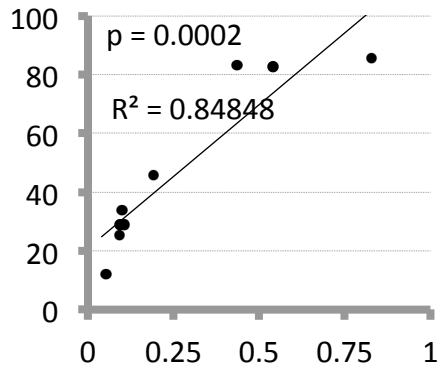
SRC_Pos.1



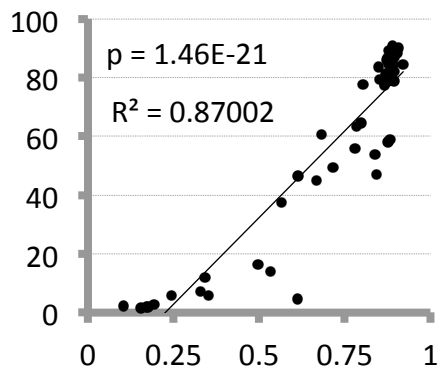
SRC_Pos.3



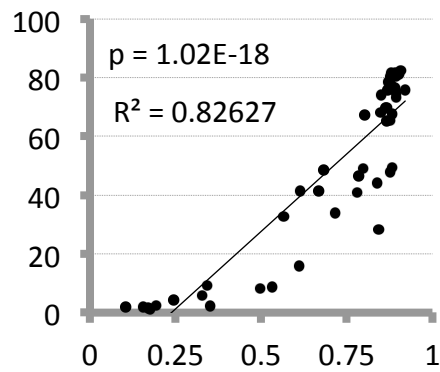
TM4SF4_Pos.2



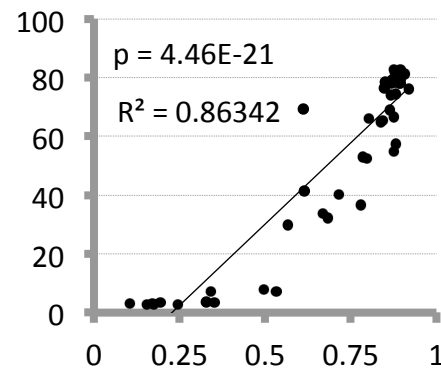
F2_Pos.1



F2_Pos.2

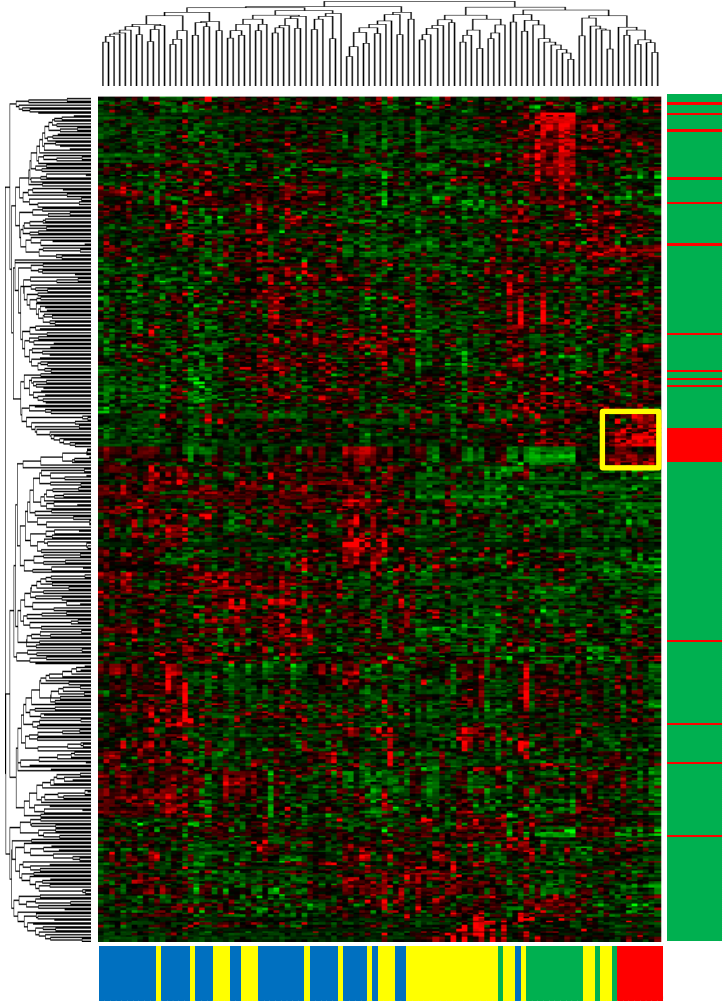


F2_Pos.3

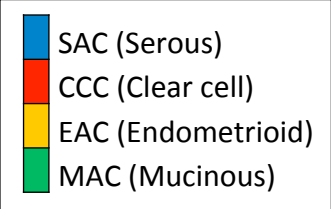
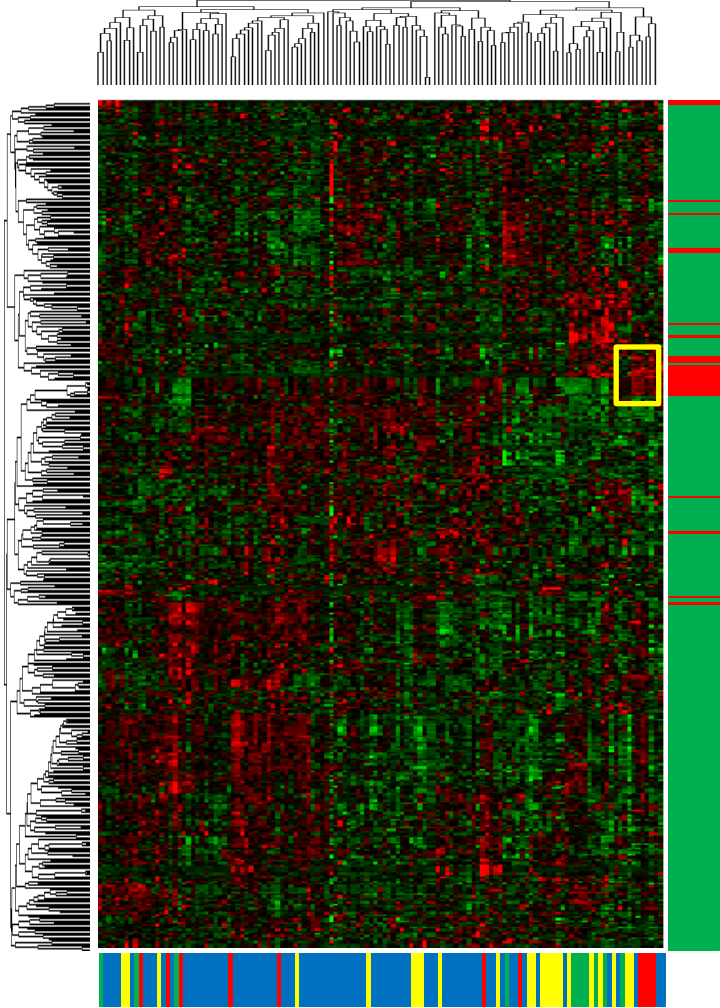


Supplementary Figure 4

a)

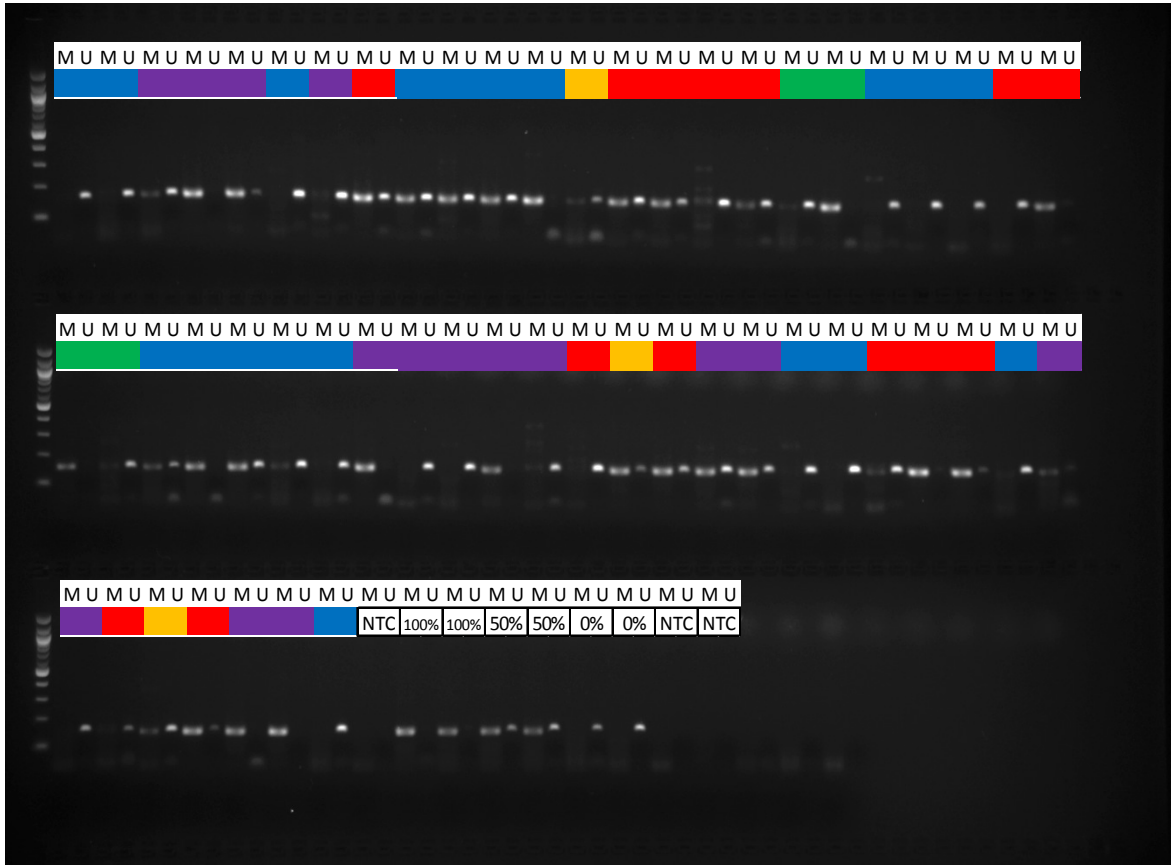
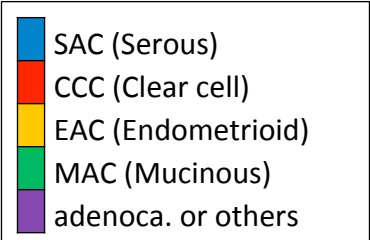
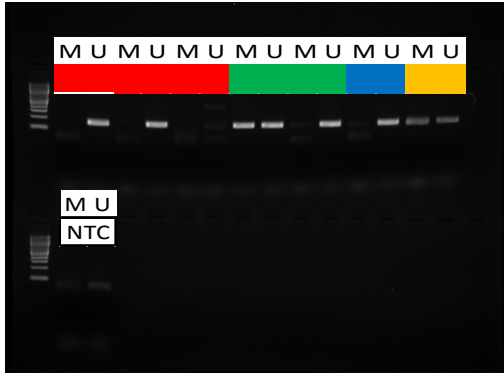


b)



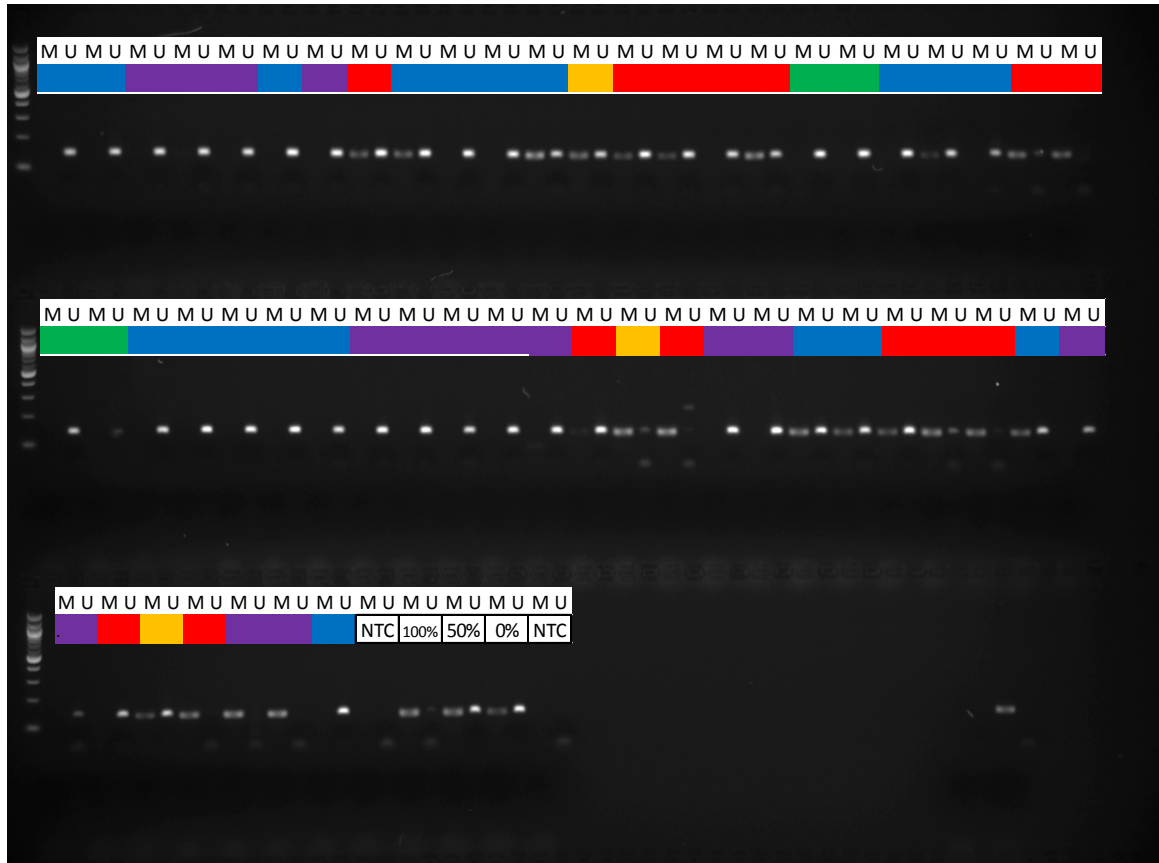
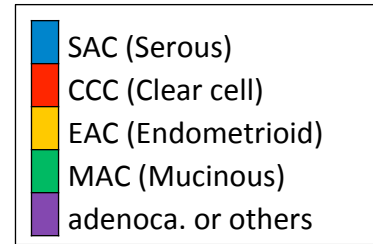
Supplementary Figure 5

a)



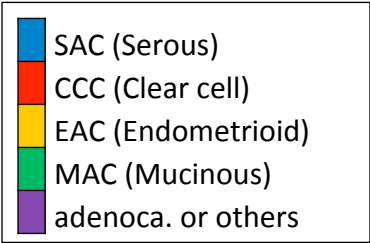
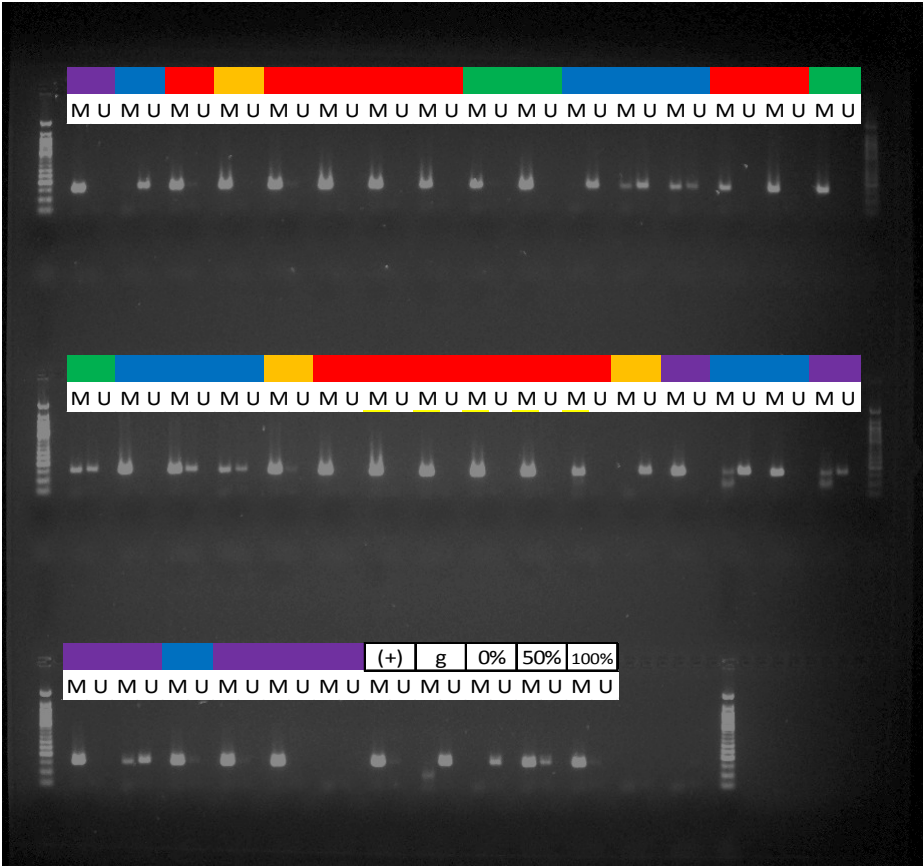
Supplementary Figure 5 (cont.)

c)



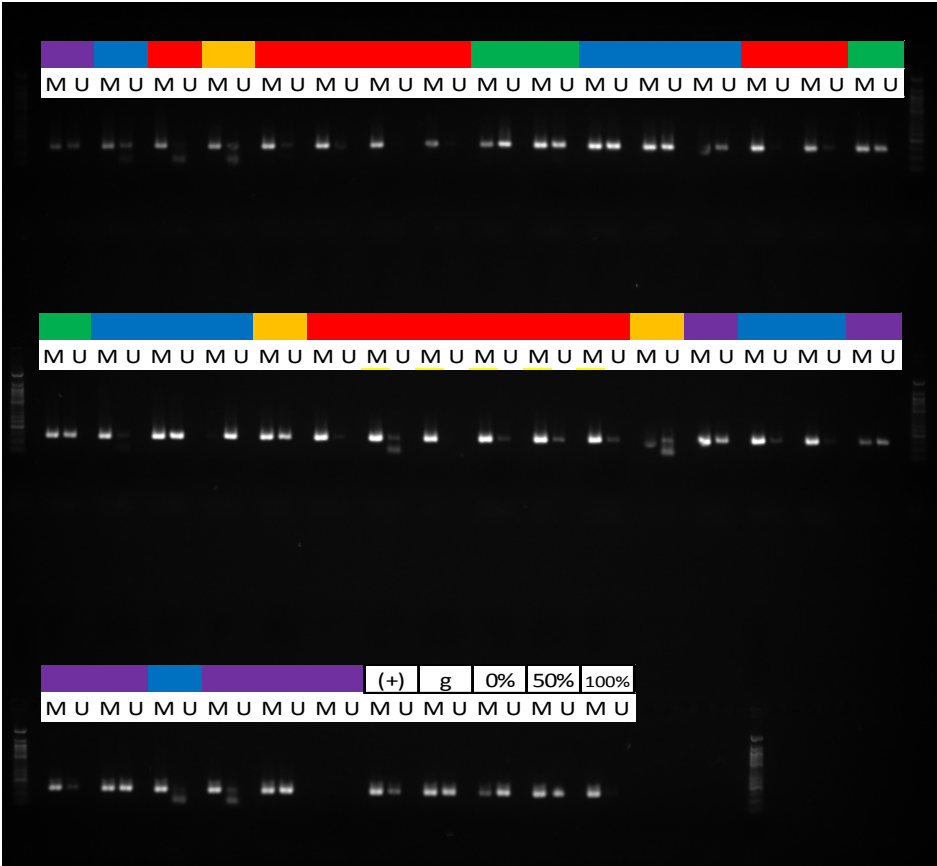
Supplementary Figure 5 (cont.)

d)



Supplementary Figure 5 (cont.)

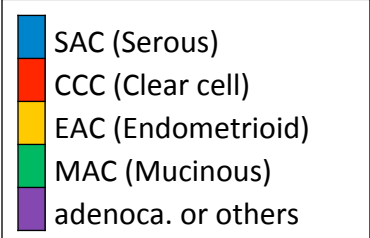
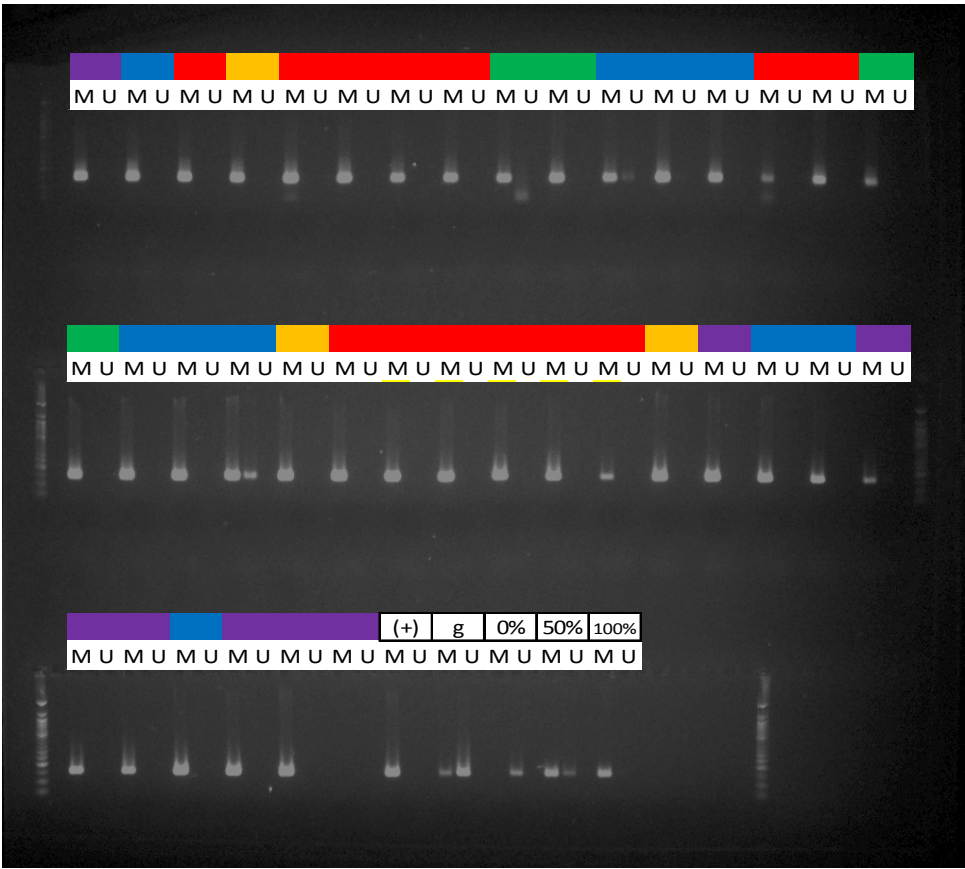
e)



- SAC (Serous)
- CCC (Clear cell)
- EAC (Endometrioid)
- MAC (Mucinous)
- adenoca. or others

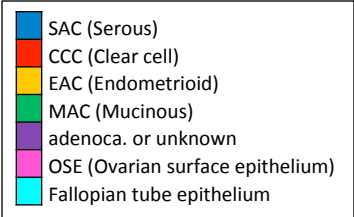
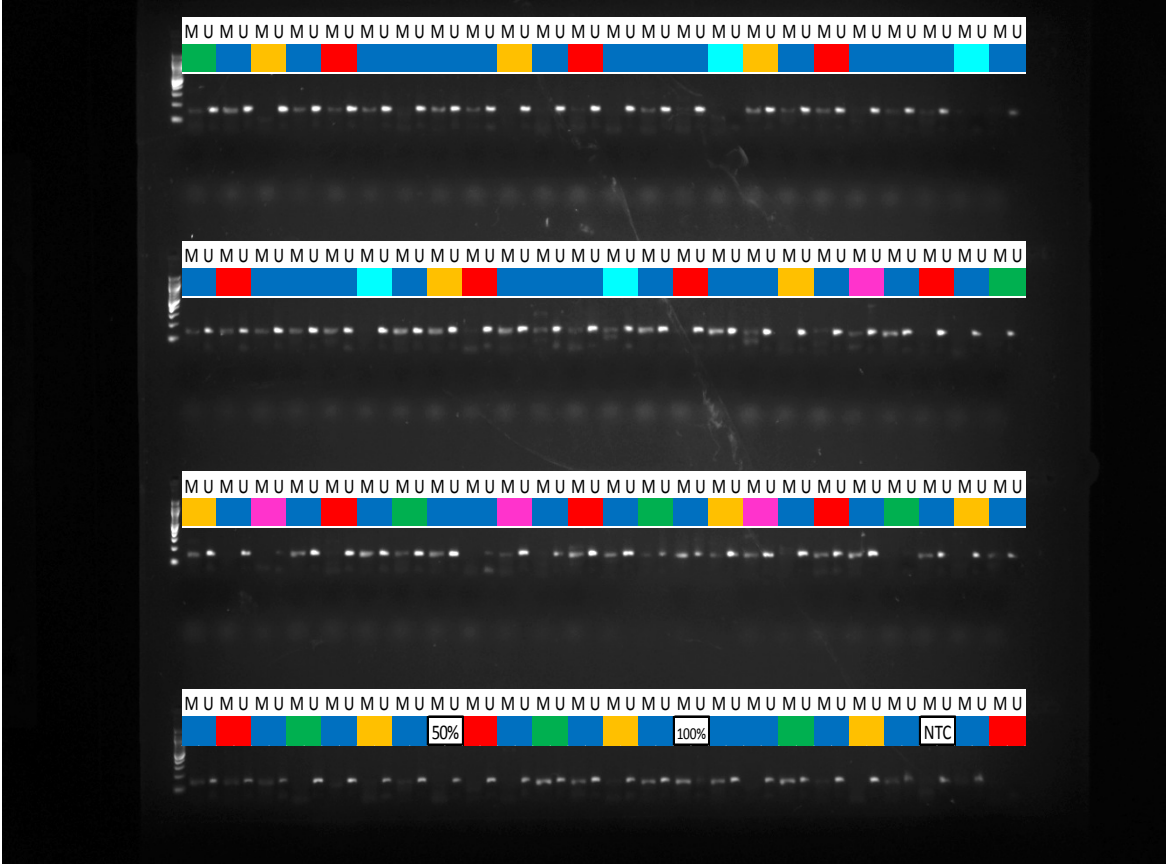
Supplementary Figure 5 (cont.)

f)



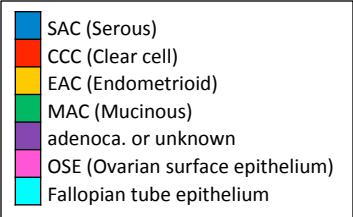
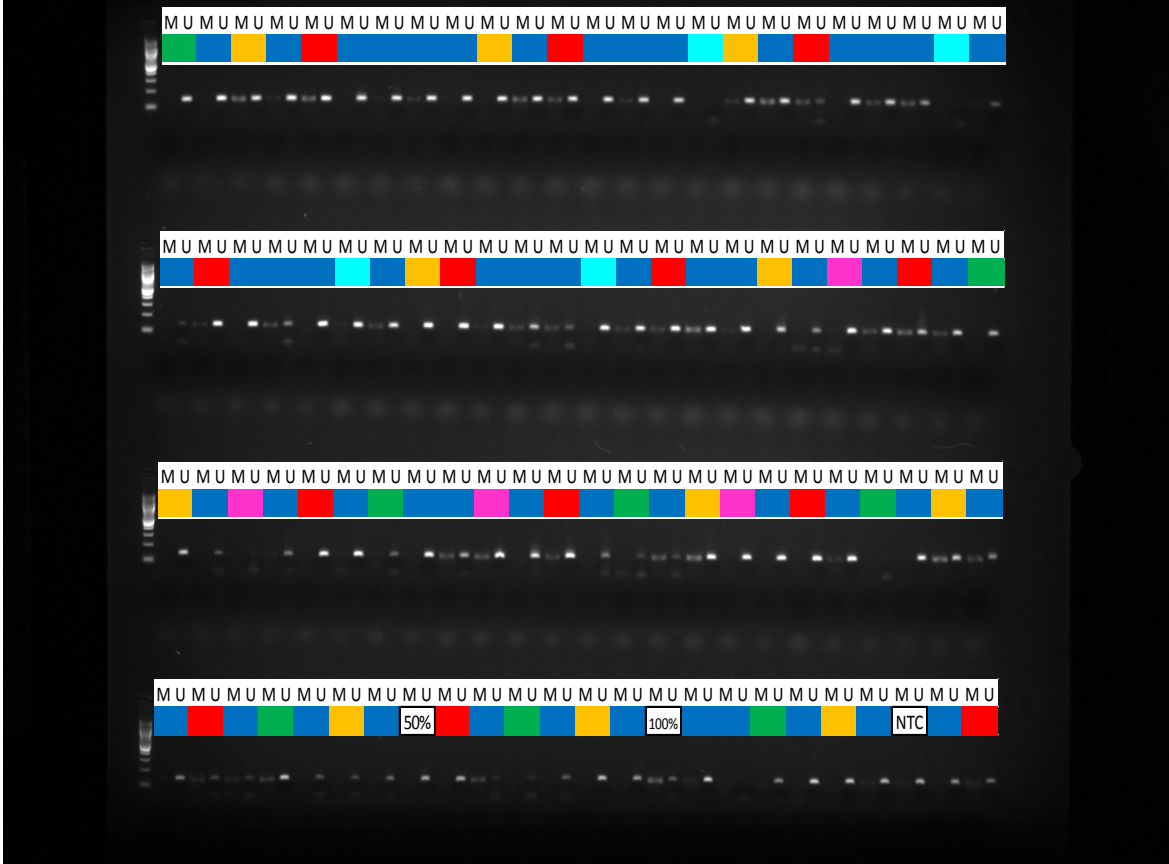
Supplementary Figure 6

a)



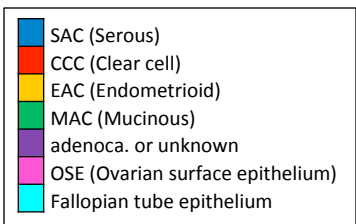
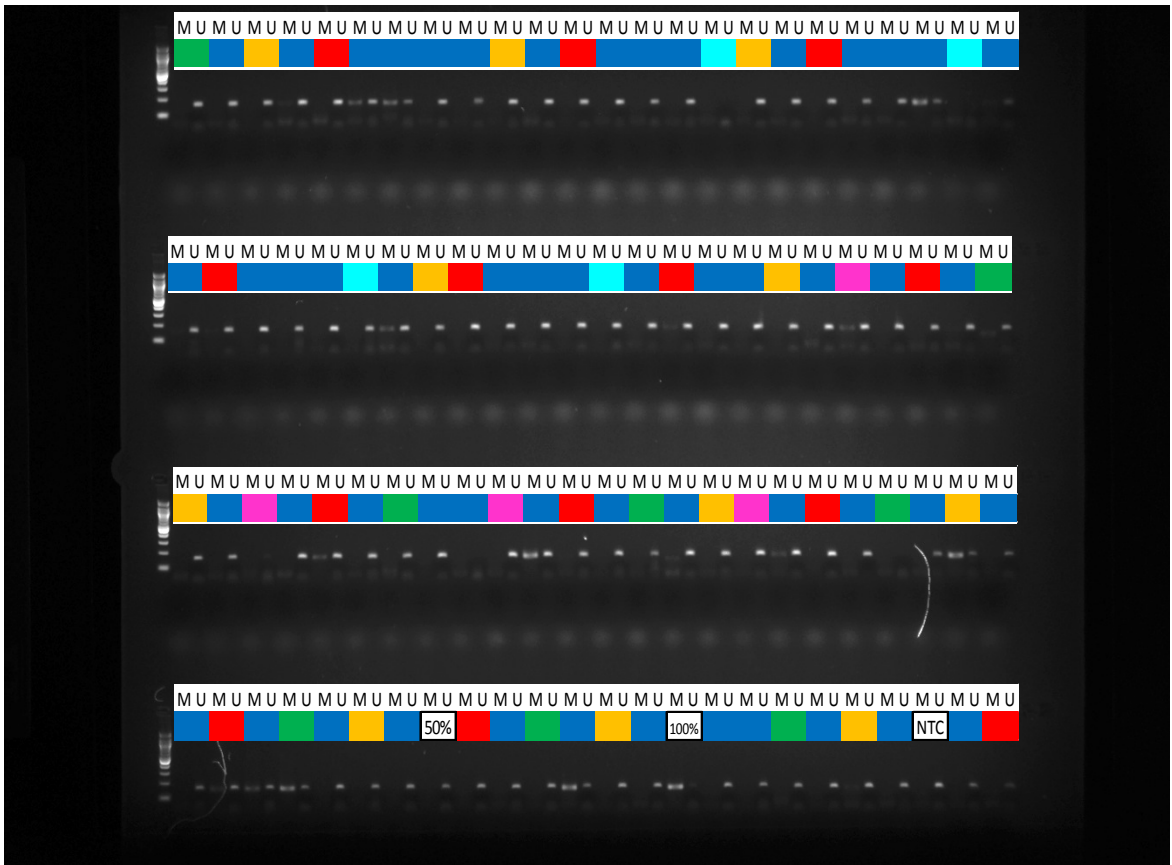
Supplementary Figure 6 (cont.)

c)



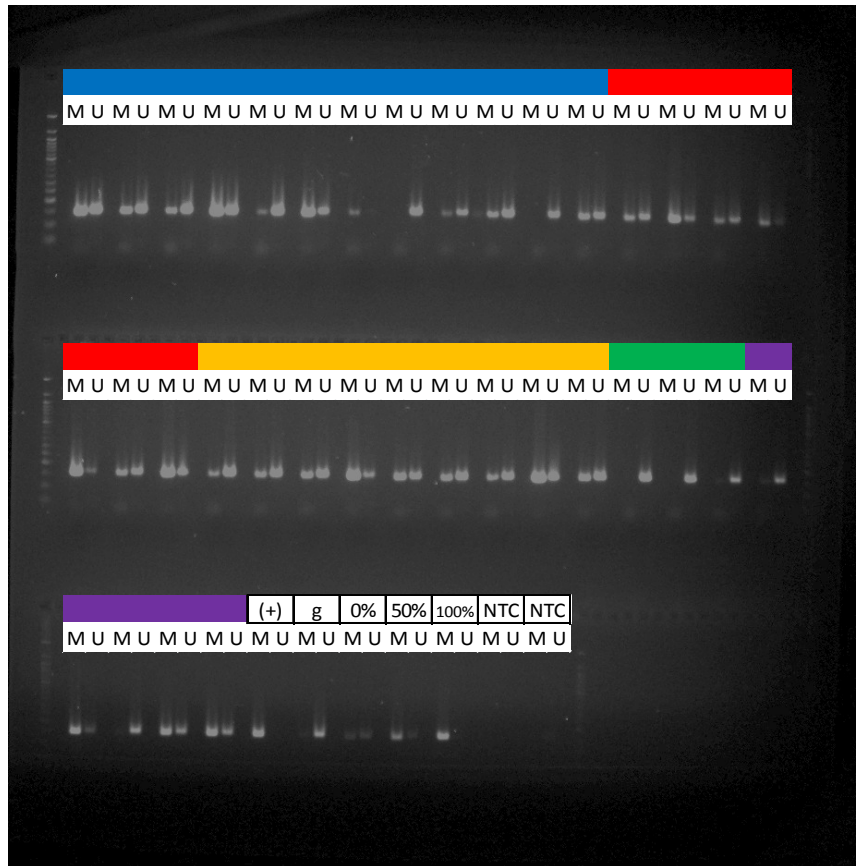
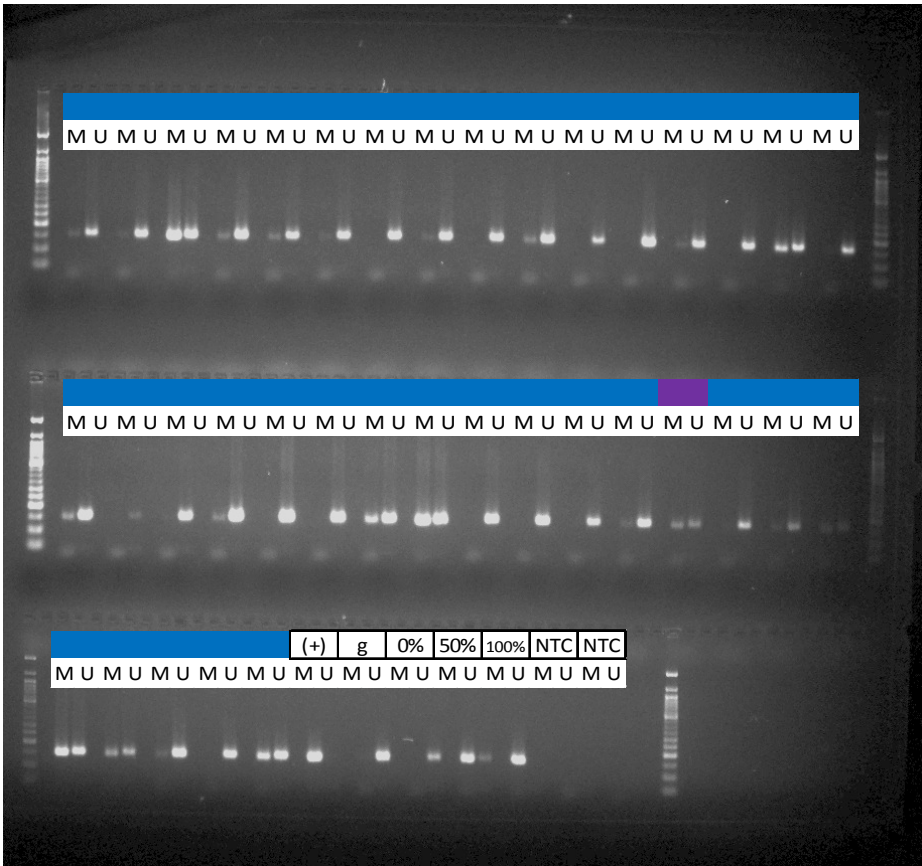
Supplementary Figure 6 (cont.)

b)



Supplementary Figure 6 (cont.)

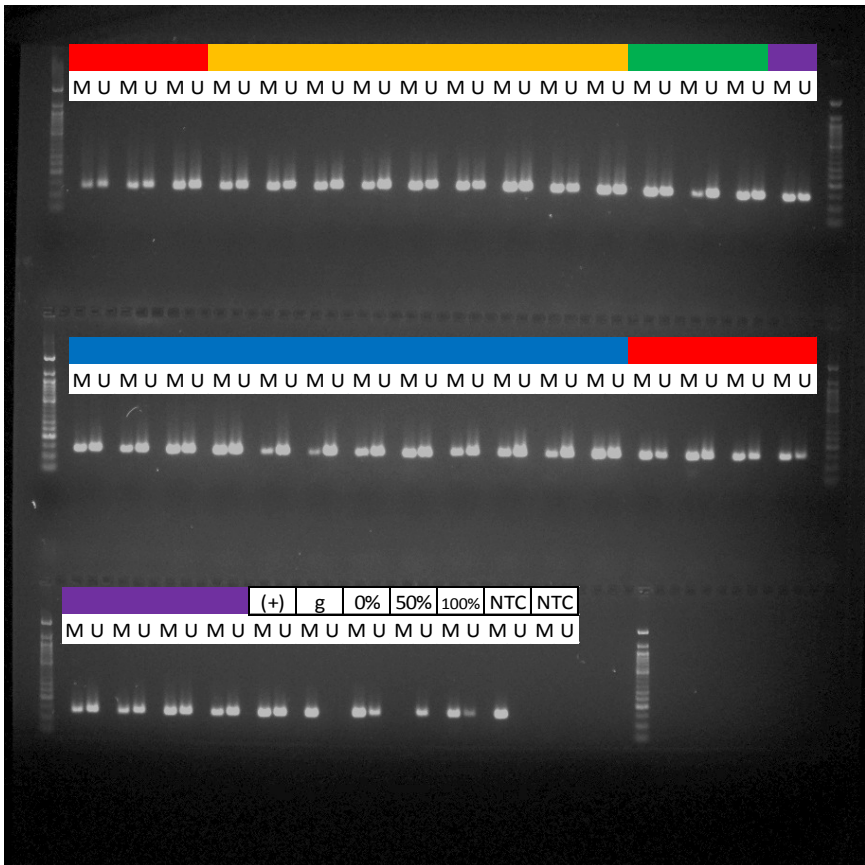
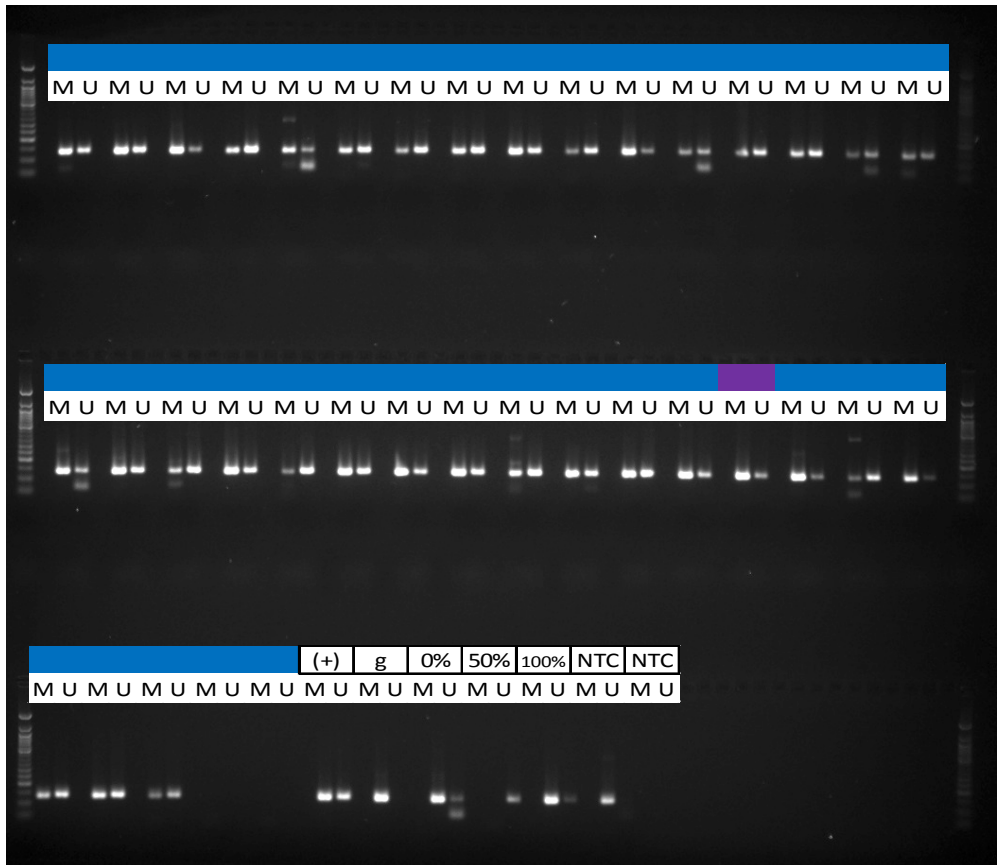
d)



- SAC (Serous)
- CCC (Clear cell)
- EAC (Endometrioid)
- MAC (Mucinous)
- adenoca. or unknown
- OSE (Ovarian surface epithelium)
- Fallopian tube epithelium

Supplementary Figure 6 (cont.)

e)



- SAC (Serous)
- CCC (Clear cell)
- EAC (Endometrioid)
- MAC (Mucinous)
- adenoca. or unknown
- OSE (Ovarian surface epithelium)
- Fallopian tube epithelium

Supplementary Figure 6 (cont.)

f)

